國立臺灣大學電機資訊學院電信工程學研究所

碩士論文

Graduate Institute of Communication Engineering
College of Electrical Engineering and Computer Science
National Taiwan University

Master Thesis

# 在多輸入多輸出循環字首系統下非冗餘盲通道估計效能提升之創新編碼器

# New Precoding For Non-Redundant Blind Channel Estimation Performance Improvement In MIMO Cyclic-Prefix Systems

陳曉峰
Hsiao-Feng Chen

指導教授：蘇柏青 博士
Advisor: Borching Su, Ph.D.

中華民國 100 年 6 月
June, 2011

# 致謝

在這兩年的時間裡，從剛開始的懵懵懂懂，到後來具有分析和獨立思考問題的能力。 首先感謝我的指導教授，蘇柏青老師。 若不是您的真知灼見，我可能會錯過如此好的論文題目; 若沒有您的細心鼓勵，我可能會迷失方向而找不到出路。 因為我們是您的第一屆學生，很多事都要您親自來教導， 真的很感謝您的付出，希望老師以後每天都可以過的很開心。

感謝MD530的夥伴們， 在平時的聊天當中， 有時會浮現一些好的靈感和解決問題的方法， 加上你們的建議和提出的問題，使得這一篇論文更趨於完善。

感謝父母一路上的陪伴與支持，沒有您們，今天的我可能就不是現在的我，也不會有現在這篇論文了。

最後，人生有時真的很奇妙，你沒想到的，它卻發生了。 你想到的，它又不一定會實現。 但我確信的是， 我從台大畢業了!

2011年 夏 台北 陳曉峰

# 中文摘要

多輸入多輸出(MIMO)區塊傳輸循環字首(CP)系統已經被證實可以達到高傳輸率，並可以簡化通道偵測和通道等化。為了要展現多輸入多輸出區塊傳輸循環字首系統的好處，我們需要準確的通道狀態資訊。為了使通道估計有更高的頻寬利用率，基於在傳輸端使用預編碼的盲通道偵測方法相較於先前的盲通道偵測方法有更多項的優勢，因而成為近來的研究對象。在這篇論文，我們提出了新一類的預編碼器，當盲通道偵測器使用我們所提出的預編碼器時，相較於使用之前研究所提出的預編碼器，可得到更為精確的通道估計。另外，我們提出一種新的方式，並藉由理論的推導和模擬的測試，發現可以用來做通道估計演算法的分析。我們也介紹了跟通道估計效能很有關聯的四個因素，其中除了雜訊因素之外，其他的因素在之前的研究裡並未被提過。我們還發現若降低這些因素，可得到更好的通道估計效能。藉由模擬，可以看出當通道偵測器採用所提出的預編碼器，相較於通道偵測器採用之前研究中所提出的預編碼器，可以得到更好的通道估計。

# Abstract

Multiple-input-multiple-output (MIMO) block transmission systems with a cyclic prefix (CP) has been proven to achieve high data rates and simplify channel estimation and equalization. In order to carry out the benefits of MIMO block transmission systems with a CP, accurate channel-state information is needed. To realize a bandwidth-efficient scheme for the channel estimation, the blind estimator based on precoding at transmitters has been recently studied due to its some advantages over other methods. In this thesis, we proposed a new class of precoders that obtains a better channel estimation performance in such estimators than previously reported precoders. In addition, we find a new way to analyze the channel estimation algorithm by theoretical derivations and numerical examples. We also introduce four factors that are potentially related to the channel estimation performance, which were not discussed in previous works except for the noise factor. We also discover that reducing the values of these factors can lead to a better channel estimation performance. Simulation results demonstrate that channel estimation using the proposed precoder indeed has a better performance than that using previously reported precoders.

# Contents

# List of Figures

# Chapter 1

# Introduction

In modern wireless communications, the high-performance transmission can be achieved by using multiple-input-multiple-output (MIMO) communication(see, e.g., [8], and references therein). However, accurate channel state information (CSI) is an essential condition to obtain high-performance transmission. The channel state information can be estimated by transmitting pilot symbols that are known to both transmitters and receivers (see, e.g., [2], and references therein). However, using the pilot symbols reduces the transmission-bandwidth efficiency. Thus, blind channel estimation has drawn considerable attention in the past few decades(see, e.g., [8],[9], and references therein).

In recent years, the second-order statistics (SOS)-based blind channel estimation algorithm has been proposed (see, e.g., [15], [11], and references therein) for either single-input-single-output systems (SISO) or MIMO systems. Among various blind channel estimation techniques, the precoding-based methods are known to be one of the major solution branches since it requires less assumption on the channel (see, e.g., [2], [5], and references therein). Lin *et al.* [7] recently proposed a channel estimation technique exploiting a periodic modulation precoding for SISO systems, and it shows better performance than previous techniques based on periodic modulation precoding in [9] and [5]. By extending the technique in [7], Wu [12] *et al.* proposed a blind channel estimation technique based on a periodic modulation precoding for SISO SC-FDE systems, and shows that the technique can obtain good estimation performance with a small number of SC-FDE symbols. In addition, a blind channel estimator for space-time coded SC-FDE systems was presented in [13]. In MIMO systems, the precoding technique has also been used for blind channel estimation (see, e.g., [4], [6], and references therein). By extending

the method in [12] to the case of spatial multiplexing MIMO block transmission systems with a cyclic prefix (CP), Shin *et al.* [10] presented a blind channel algorithm based on a simplified non-redundant precoding for MIMO systems. In addition, they also established the conditions required for the simplified precoding to enable blind MIMO channel identification. In their simulations, the channel MSE performance of the estimator in [10] is compared with that of the cyclo-stationary statistics based estimator in [2] and the subspace-based estimator in [1]. It shows better performance than the estimator in [2] and [1]. Moreover, Chen *et al.* [3] presented a semiblind channel algorithm that is also based on periodic precoding for MIMO SC-FDE systems. The difference is that the size of the precoding matrix can be even or odd, thus relaxing the size requirement in [10] and [14].

In [10], an optimal simplified precoding based on the sense of minimizing the impact of unknown additive noise is derived. Further, the channel estimation was done based on the assumption that the autocorrelation matrix of the received signal can be exactly estimated. However, in practice such accurate information on the autocorrelation matrix can not be obtained unless the number of received symbol blocks is infinite. Therefore, the optimal precoding presented in [10] may not leads to the best channel estimation performance unless the number of received symbol blocks is infinite. This limits the applicability of the method in [10] in practical situations.

In this thesis, we proposed a new class of precoders that further improves the performance of the aforementioned blind channel estimation algorithm. We also introduce some factors that potentially affect the channel estimation, including the noise. The derivation of the optimal precoder in [10] only considered minimizing the impact of the noise, but ignored other factors by the assumption that the number of received blocks is infinite. Therefore, there can potentially be some precoders that can achieve a better performance as long as the number of symbol blocks is finite. The simulation results show that the proposed precoder results in a better channel estimation performance than that in [10].

This rest of the thesis is organized as follows. Chapter 2 presents the system model of MIMO block transmission with a CP. Chapter 3 first reviews a blind channel estimation technique using a systematic precoding, previously reported in [10], and then proposes a new class of precoders that facilitates the aforementioned channel estimator to get more accurate channel estimation performance than that in [10]. Chapter 4 analyzes the channel

estimation performance from the theoretical point of view, and shows how some factors other than the noise that are not previously known affect the channel estimation performance. Chapter 5 shows and explains the simulation results. Chapter 6 concludes this thesis.

The following notations are used in this thesis. Bold uppercase is used for matrices, and bold lowercase is used for vectors. Transpose, complex conjugate, Hermitian, and inverse of matrix $\mathbf{A}$ are represented by $\mathbf{A}^T$, $\mathbf{A}^*$, $\mathbf{A}^\dagger$, and $\mathbf{A}^{-1}$, respectively. $\otimes$ represents the Kronecker product, $\mathbf{I}_m$ is the $m \times m$ matrix , $\mathbf{1}_m$ is a $m \times 1$ vector with all ones, diag(**x**) stands for a diagonal matrix with **x** on its diagonal, and tr($\mathbf{A}$) denotes the trace operation. $E(.)$ is the statistic expectation. The $M \times M$ matrix $\mathbf{A}^{1/2}$ equals to $\mathbf{U}\text{diag}[\sqrt{\lambda_1}\sqrt{\lambda_2}...\sqrt{\lambda_M}]\mathbf{U}^\dagger$, where $\mathbf{U}$ is a unitary matrix corresponding to eigenvectors of $\mathbf{A}$ and $\lambda_i$ is the $i$th eigenvalue of $\mathbf{A}$. $\mathbf{A}[:, j]$ represents the $j$th column of the matrix $\mathbf{A}$, and $\mathbf{A}[i_1 : i_2, j_1 : j_2]$ denotes a submatrix obtained by extracting rows $i_1$ to $i_2$ and columns $j_1$ to $j_2$ from the matrix $\mathbf{A}$. $\mathcal{CN}(0, \sigma^2)$ represents a circular symmetric complex Gaussian distribution with zero mean and variance $\sigma^2$.

# Chapter 2

# System Model for MIMO Block transmission with a cyclic prefix

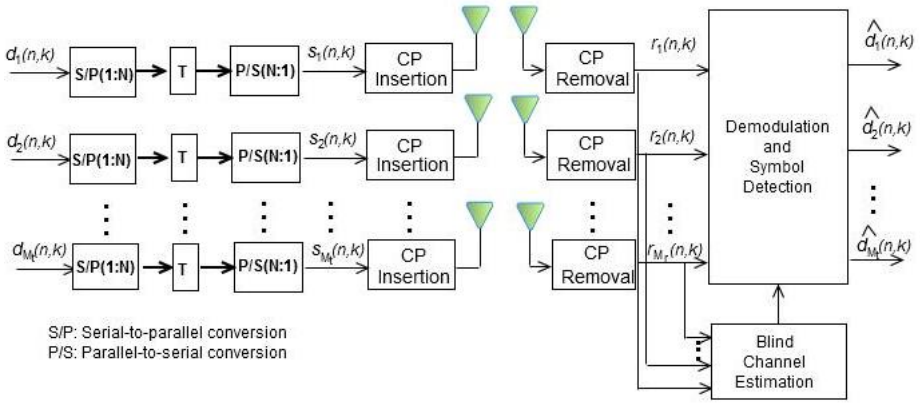


Figure 2.1: MIMO block transmission system with a cyclic prefix which has $M_t$ transmit and $M_r$ receive antennas.

Consider a multiple-input-multiple-output (MIMO) block transmission system with a cyclic prefix (CP) [10], equipped with $M_t$ transmit and $M_r$ receive antennas as illustrated in Fig. 2.1. As seen in the figure, $\mathbf{d}(n,k)$ denotes the information symbol vector as

$$\mathbf{d}(n,k) \triangleq [d_1(n,k)\ d_2(n,k)\ ...\ d_{M_t}(n,k)]^T \tag{2.1}$$

where $d_i(n,k)$ is the information symbol loaded at the $k$th subcarrier of the $n$th symbol block in the $i$th transmit antenna. By stacking $\mathbf{d}(n,k)$ with $0 \leqslant k \leqslant N-1$, we denote the $NM_t \times 1$ vector $\mathbf{d}(n)$ as

$$\mathbf{d}(n) \triangleq [\mathbf{d}(n,0)^T\ \mathbf{d}(n,1)^T\ ...\ \mathbf{d}(n,N-1)^T]^T \tag{2.2}$$

where $N$ is the size of a symbol block. By applying a $N \times N$ precoding matrix $\mathbf{T}$ to information symbols at each transmit antenna, the transformed signal vector $\mathbf{s}(n)$ at $M_t$ transmit antennas is given as

$$\begin{aligned} \mathbf{s}(n,k) &\triangleq [s_1(n,k)\ s_2(n,k)\ ...\ s_{M_t}(n,k)]^T & (2.3)\\ \mathbf{s}(n) &\triangleq [\mathbf{s}(n,0)^T\ \mathbf{s}(n,1)^T\ ...\ \mathbf{s}(n,N-1)^T]^T \\ &= (\mathbf{T} \otimes \mathbf{I}_{M_t})\mathbf{d}(n). & (2.4) \end{aligned}$$

Then, we copy the last $PM_t$ components of the vector $\mathbf{s}(n)$, which we called CP. We insert the CP in front of $\mathbf{s}(n)$ as

$$\mathbf{s}_{cp}(n) \triangleq [\mathbf{s}(n,N-P)^T\ ...\ \mathbf{s}(n,N-1)^T\mathbf{s}(n,0)^T\ ...\ \mathbf{s}(n,N-1)^T]^T \tag{2.5}$$

where $P$ is the length of the CP at each transmit antenna, and is set to be equal to or larger than a MIMO channel order to avoid inter-block interference (IBI). Let us consider an $M_t \times M_r$ finite-impulse response (FIR) MIMO channel with $L$ as the upper bound on the channel order, and $\mathbf{H}(l)$ is the $l$th lag of the MIMO channel.

At the receiver, we remove the CP portion corrupted by IBI after the $n$th symbols is received. The received signal vector $\mathbf{r}(n)$ is given as

$$\begin{aligned} \mathbf{r}(n,k) &\triangleq [r_1(n,k)\ r_2(n,k)\ ...\ r_{M_r}(n,k)]^T & (2.6)\\ \mathbf{r}(n) &\triangleq [\mathbf{r}(n,0)^T\ \mathbf{r}(n,1)^T\ ...\ \mathbf{r}(n,N-1)^T]^T \\ &= \mathcal{H}\mathbf{s}(n) + \boldsymbol{\eta}(n) & (2.7) \end{aligned}$$

where $\boldsymbol{\eta}(n)$ is the $NM_r \times 1$ additive white Gaussian noise (AWGN) vector, and $\mathcal{H}$ is a block circulant matrix with $[\mathbf{H}(0)^T\mathbf{H}(1)^T\ ...\ \mathbf{H}(L)^T\mathbf{0}^T\ ...\ \mathbf{0}^T]^T$ being its first column block.

In [10], a method to blindly estimate the MIMO channel matrices $\mathbf{H}(l)$ was developed, using the second-order statistics of the received symbol blocks. As seen in Fig. 2.1, if we let $\mathbf{T}$ be the $N \times N$ inverse discrete Fourier transform (IDFT) matrix, this system reduces to a MIMO-OFDM system. In addition, if we set $\mathbf{T}$ to be equal to $\mathbf{I_N}$, this system turns into a MIMO single-carrier frequency-domain equalization (SC-FDE) system. Besides, when $\mathbf{T}\mathbf{T}^\dagger = \mathbf{\Omega} \neq \mathbf{I}$, the system is a MIMO-OFDM or MIMO SC-FDE system with precoding [10].

Since we use the second-order statistics method to do the channel estimation, the autocorrelation matrix of the received vector $\mathbf{r}(n)$ is defined as $\mathbf{R_{rr}} \triangleq E(\mathbf{r}(n)\mathbf{r}(n)^\dagger)$ which has the term $\mathbf{T}\mathbf{T}^\dagger$. Let $\mathbf{T}\mathbf{T}^\dagger = \mathbf{\Omega}$ , and we need to design the matrix $\mathbf{\Omega}$ appropriately such that the estimation error of the MIMO channel matrices $\mathbf{H}(l)$ could be as small as possible. The matrix $\mathbf{T}$ can be expressed as $\mathbf{\Omega}^{1/2}\mathbf{U_T}$ with $\mathbf{\Omega} = \mathbf{\Omega}^{1/2}\mathbf{\Omega}^{(1/2)^\dagger}$, where $\mathbf{U_T}$ is a unitary matrix.

In the next chapter, we will describe a blind channel estimation scheme for the MIMO-CP systems described here.

# Chapter 3

# Precoding-Based Blind Channel Estimation

In this chapter, we study a blind channel estimation scheme for MIMO-CP systems based on precoding techniques. We will first review the method proposed in [10] and then propose a new class of precoding matrices that further improve the channel estimation performance.

## 3.1 Blind channel estimation exploiting the precoding matrix

In this section, we describe the blind channel estimation algorithm based on a simplified systematic precoding for the MIMO block system in Chapter 2. Before going into the details of the estimation technique, we make the following assumptions.

**1)** The $(L+1)M_r \times M_t$ matrix $\mathbf{H}$ is defined as $[\mathbf{H}(0)^T\mathbf{H}(1)^T ... \mathbf{H}(L)^T]^T$ which has full column rank, i.e., rank($\mathbf{H}$)= $M_t$.

**2)** The information symbol $d_j(n,k)$ is spatially and temporally uncorrelated with other information symbols, i.e., $E(d_j(n_1,k_1)d_i^*(n_2,k_2)) = \sigma_d^2\delta(j-i)\delta(n_1-n_2)\delta(k_1-k_2)$. The AWGN is zero mean and uncorrelated both spatially and temporally, i.e., $E(\boldsymbol{\eta}(m)\boldsymbol{\eta}(n)^\dagger) = \sigma_\eta^2\delta(m-n)\mathbf{I}_{NM_r}$. In addition, the information symbols is uncorrelated with the AWGN, i.e., $E(\mathbf{d}(n)\boldsymbol{\eta}(n)^\dagger) = \mathbf{0}$.

To describe the precoding-based blind estimation technique proposed in [10], we first define the $N \times N$ matrix $\mathbf{\Pi}$ as

$$\mathbf{\Pi} = \begin{bmatrix} \mathbf{0} & 1 \\ \mathbf{I}_{N-1} & \mathbf{0} \end{bmatrix} \tag{3.1}$$

and define $\mathbf{\Pi}^0$ as $\mathbf{I}_N$. Then, we can rewrite the $NM_r \times NM_t$ block circulant channel matrix $\mathcal{H}$ as

$$\mathcal{H} \;=\; \sum_{i=0}^{L} \mathbf{\Pi}^i \otimes \mathbf{H}(i). \tag{3.2}$$

Thus, the $NM_r \times 1$ received vector $\mathbf{r}(n)$ can be written as

$$\begin{aligned} \mathbf{r}(n) &= (\sum_{i=0}^{L} \mathbf{\Pi}^i \otimes \mathbf{H}(i))(\mathbf{T} \otimes \mathbf{I}_{M_t})\mathbf{d}(n) + \boldsymbol{\eta}(n) \\ &= (\sum_{i=0}^{L} \mathbf{\Pi}^i \mathbf{T} \otimes \mathbf{H}(i))\mathbf{d}(n) + \boldsymbol{\eta}(n). \end{aligned} \tag{3.3}$$

We assume the signal power $\sigma_d^2 = 1$, and denote the noise power as $\sigma_\eta^2$. In addition, we defined the SNR as $\triangleq \sigma_d^2/\sigma_\eta^2$. The autocorrelation matrix of $\mathbf{r}(n)$ is given as

$$\begin{aligned} \mathbf{R_{rr}} &\triangleq E(\mathbf{r}(n)\mathbf{r}(n)^\dagger) \\ &= \mathcal{H}(\mathbf{\Omega} \otimes \mathbf{I}_{M_t})\mathcal{H}^\dagger + \sigma_\eta^2 \mathbf{I}_{NM_r} \\ &= \sum_{i=0}^{L}\sum_{j=0}^{L} \mathbf{\Pi}^i \mathbf{\Omega} (\mathbf{\Pi}^T)^j \otimes \mathbf{H}(i)\mathbf{H}(j)^\dagger + \sigma_\eta^2 \mathbf{I}_{NM_r}\ . \end{aligned} \tag{3.4}$$

Based on the simplified systematic precoding, the $N \times N$ matrix $\mathbf{\Omega}$ was developed in [10], and it was given as

$$\mathbf{\Omega} = \begin{bmatrix} \mathbf{D}_{\xi_1} & \mathbf{D}_\rho \\ \mathbf{D}_\rho & \mathbf{D}_{\xi_2} \end{bmatrix}, \tag{3.5}$$

$$\begin{aligned} &\mathbf{D}_{\boldsymbol{\xi_1}} = \text{diag}([\xi(0)\ \xi(1) \ldots\ \xi(N/2-1)]), \\ &\mathbf{D}_{\boldsymbol{\xi_2}} = \text{diag}([\xi(N/2)\ \xi(N/2+1) \ldots\ \xi(N-1)]), \\ &\mathbf{D}_\rho = \text{diag}([\rho(0)\ \rho(1) \ldots\ \rho(N/2-1)]), \end{aligned} \tag{3.6}$$

where $N$ is assumed to be an even number with $N \geq 4L+2$ , $\rho(m)$ are real numbers, and $\sum_{m=0}^{N-1}\xi(m)+\sum_{m=N-P}^{N-1}\xi(m)=N+P$ since we need to preserve the signal power per symbol block including the CP after the transformation by $\mathbf{T}$ [10]. In the following, we present how to obtain the MIMO channel $\mathbf{H}$ from $\mathbf{R_{rr}}$ in detail.

The $NM_r \times NM_r$ matrix $\mathbf{R_{rr}}$ is partitioned as

$$\mathbf{R}(m,n) \triangleq \mathbf{R_{rr}}[mM_r+1:(m+1)M_r, nM_r+1:(n+1)M_r], 0 \leqslant m,n < N. \quad (3.7)$$

Let us denote $\mathbf{\Lambda}_i(\mathbf{R_{rr}})$ $(\mathbf{\Lambda}_{-i}(\mathbf{R_{rr}}))$, and $\mathbf{\Lambda}_i(\mathbf{HH}^\dagger)$ $(\mathbf{\Lambda}_{-i}(\mathbf{HH}^\dagger))$ as the matrix composed of the $M_r \times M_r$ submatrices on the $i$th upper (lower) block diagonal of $\mathbf{R_{rr}}$ and $\mathbf{HH}^\dagger$, which are given by

$$\begin{aligned}
\mathbf{\Lambda}_i(\mathbf{R_{rr}}) &\triangleq [\mathbf{R_{rr}}(0,i)^T\ \mathbf{R_{rr}}(1,1+i)^T\ ...\ \mathbf{R_{rr}}(N-1-i,N-1)^T]^T \\
\mathbf{\Lambda}_{-i}(\mathbf{R_{rr}}) &\triangleq [\mathbf{R_{rr}}(i,0)^T\ \mathbf{R_{rr}}(1+i,1)^T\ ...\ \mathbf{R_{rr}}(N-1,N-1-i)^T]^T \\
\mathbf{\Lambda}_i(\mathbf{HH}^\dagger) &\triangleq [\mathbf{H}(i)^*\mathbf{H}(0)^T\ \mathbf{H}(i+1)^*\mathbf{H}(1)^T ...\ \mathbf{H}(L)^*\mathbf{H}(L-i)^T]^T \\
\mathbf{\Lambda}_{-i}(\mathbf{HH}^\dagger) &\triangleq [\mathbf{H}(0)^*\mathbf{H}(i)^T\ \mathbf{H}(1)^*\mathbf{H}(i+1)^T ...\ \mathbf{H}(L-i)^*\mathbf{H}(L)^T]^T. \qquad (3.8)
\end{aligned}$$

To obtain the channel-product matrices $\mathbf{HH}^\dagger$ from the autocorrelation matrix $\mathbf{R_{rr}}$ in (3.4). We can express $[\mathbf{\Lambda}_{N/2}(\mathbf{R_{rr}})^T\mathbf{\Lambda}_{-N/2}(\mathbf{R_{rr}})^T\mathbf{\Lambda}_0(\mathbf{R_{rr}})^T]^T$ and
$[\mathbf{\Lambda}_{N/2+i}(\mathbf{R_{rr}})^T\mathbf{\Lambda}_{-N/2+i}(\mathbf{R_{rr}})^T\mathbf{\Lambda}_i(\mathbf{R_{rr}})^T\mathbf{\Lambda}_{-N+i}(\mathbf{R_{rr}})^T]^T$ as, respectively

$$\begin{aligned}
[\mathbf{\Lambda}_{N/2}(\mathbf{R_{rr}})^T\mathbf{\Lambda}_{-N/2}(\mathbf{R_{rr}})^T\mathbf{\Lambda}_0(\mathbf{R_{rr}})^T]^T &= ([\mathbf{A}_0^T\ \mathbf{A}_0^T\ \mathbf{B}_0^T]^T \otimes \mathbf{I}_{M_r})\mathbf{\Lambda}_0(\mathbf{HH}^\dagger) \\
&+ \sigma_\eta^2[\mathbf{0}_N\ \mathbf{1}_N]^T \otimes \mathbf{I}_{M_r} \qquad (3.9)
\end{aligned}$$

$$\begin{aligned}
&[\mathbf{\Lambda}_{N/2+i}(\mathbf{R_{rr}})^T\mathbf{\Lambda}_{-N/2+i}(\mathbf{R_{rr}})^T\mathbf{\Lambda}_i(\mathbf{R_{rr}})^T\mathbf{\Lambda}_{-N+i}(\mathbf{R_{rr}})^T]^T \\
= \quad &([\mathbf{A}_i^T\ \mathbf{A}_i^T\ \mathbf{B}_i^T]^T \otimes \mathbf{I}_{M_r})\mathbf{\Lambda}_i(\mathbf{HH}^\dagger) \text{ for } 1 \leq i \leq L.
\end{aligned}$$

(3.10)

In (3.9) and (3.10), the $N/2 \times (L-i+1)$ matrix $\mathbf{A}_i$ for $0 \leq i \leq L$ and the $N \times (L-i+1)$ matrix $\mathbf{B}_i$ for $0 \leq i \leq L$ are defined as, respectively

$$\mathbf{A}_i = \begin{bmatrix} \rho(0) & \rho(N/2-1) & ... & \rho(N/2-L+i) \\ \rho(1) & \rho(0) & ... & \rho(N/2-L+i+1) \\ . & . & ... & . \\ . & . & ... & . \\ . & . & ... & . \\ \rho(N/2-1) & \rho(N/2-2) & ... & \rho(N/2-(L-i+1)) \end{bmatrix} \tag{3.11}$$

$$\mathbf{B}_i = \begin{bmatrix} \xi(0) & \xi(N-1) & ... & \xi(N-L+i) \\ \xi(1) & \xi(0) & ... & \xi(N-L+i+1) \\ . & . & ... & . \\ . & . & ... & . \\ . & . & ... & . \\ \xi(N-1) & \xi(N-2) & ... & \xi(N-(L-i+1)) \end{bmatrix}. \tag{3.12}$$

Let $\mathbf{C}_i$ be the pseudoinverse matrix of $[\mathbf{A}_i^T \ \mathbf{A}_i^T \ \mathbf{B}_i^T]^T \otimes \mathbf{I}_{M_r}$. So, $\mathbf{C}_i$ can be written as

$$\mathbf{C}_i = (2\mathbf{A}_i^T\mathbf{A}_i + \mathbf{B}_i^T\mathbf{B}_i)^{-1}[\mathbf{A}_i^T \ \mathbf{A}_i^T \ \mathbf{B}_i^T] \otimes \mathbf{I}_{M_r}, \text{ for } i = 0 \ ... \ L. \tag{3.13}$$

If $2\mathbf{A}_i^T\mathbf{A}_i + \mathbf{B}_i^T\mathbf{B}_i$ is invertible, we can obtain $\mathbf{\Lambda}_i(\mathbf{H}\mathbf{H}^\dagger)$ for $0 \leq i \leq L$. Since both $\mathbf{A}_i^T\mathbf{A}_i$ and $\mathbf{B}_i^T\mathbf{B}_i$ are positive semidefinite matrices, it is guaranteed to be nonsingular if $\mathbf{A}_i$ or $\mathbf{B}_i$ has full column rank. If the matrix $\mathbf{C}_i$ is obtained, the estimate of $\mathbf{\Lambda}_i(\mathbf{H}\mathbf{H}^\dagger)$ are obtained as, respectively

$$\begin{aligned} \mathbf{\Lambda}_0(\tilde{\mathbf{H}}\tilde{\mathbf{H}}^\dagger) &= \mathbf{C}_0[\mathbf{\Lambda}_{N/2}(\mathbf{R_{rr}})^T\mathbf{\Lambda}_{-N/2}(\mathbf{R_{rr}})^T\mathbf{\Lambda}_0(\mathbf{R_{rr}})^T]^T \\ &= \mathbf{\Lambda}_0(\mathbf{H}\mathbf{H}^\dagger) + \mathbf{C}_0(\sigma_\eta^2[\mathbf{0}_N \ \mathbf{1}_N]^T \otimes \mathbf{I}_{M_r}) \end{aligned} \tag{3.14}$$

$$\begin{aligned} \mathbf{\Lambda}_i(\tilde{\mathbf{H}}\tilde{\mathbf{H}}^\dagger) &= \mathbf{C}_i[\mathbf{\Lambda}_{N/2+i}(\mathbf{R_{rr}})^T\mathbf{\Lambda}_{-N/2+i}(\mathbf{R_{rr}})^T\mathbf{\Lambda}_i(\mathbf{R_{rr}})^T\mathbf{\Lambda}_{-N+i}(\mathbf{R_{rr}})^T]^T \\ &= \mathbf{\Lambda}_i(\mathbf{H}\mathbf{H}^\dagger), \text{ for } i = 1 \ ... \ L. \end{aligned} \tag{3.15}$$

Using $\mathbf{\Lambda}_i(\tilde{\mathbf{H}}\tilde{\mathbf{H}}^\dagger)$, $0 \leqslant i \leqslant L$, we can construct the matrix $\tilde{\mathbf{H}}\tilde{\mathbf{H}}^\dagger$. When we take the eigenvalue decomposition of $\tilde{\mathbf{H}}\tilde{\mathbf{H}}^\dagger$, the matrix $\tilde{\mathbf{H}}\tilde{\mathbf{H}}^\dagger$ can be written as

$$\tilde{\mathbf{H}}\tilde{\mathbf{H}}^\dagger = \mathbf{U}\text{diag}[\lambda_1 \ \lambda_2 ... \ \lambda_{(L+1)M_r}]\mathbf{U}^\dagger \tag{3.16}$$

where $\mathbf{U}$ is a $(L+1)M_r \times (L+1)M_r$ unitary matrix corresponding to eigenvectors and $\lambda_i$ is the $i$th eigenvalue. In (3.16), the eigenvalues are considered to be in decreasing order. Since rank($\mathbf{H}$) = $M_t$ by assumption 1, we have $\lambda_i > 0$ for $1 \leq i \leq M_t$ and $\lambda_i = 0$ for $M_t + 1 \leq i \leq (L+1)M_r$. Thus, the estimated MIMO channel $\check{\mathbf{H}}$ is obtained as

$$\check{\mathbf{H}} = \mathbf{U}[:, 1 : M_t]\text{diag}[\sqrt{\lambda_1}\ \sqrt{\lambda_2}\ ...\ \sqrt{\lambda_{M_t}}]\mathbf{V}^\dagger \tag{3.17}$$

where the $M_t \times M_t$ matrix $\mathbf{V}^\dagger$ is an arbitrary unitary matrix that represents a MIMO channel ambiguity inherent in blind channel estimation techniques. If the matrix $\mathbf{R_{rr}}$ is only corrupted by the additive noise, we can improve the channel estimation by subtracting $\frac{1}{M_r(L+1)-M_t}\sum_{j=M_t+1}^{(L+1)M_r}\lambda_j$ from $\lambda_i$ for $1 \leqslant i \leqslant M_t$ [10]. In other words, the adjusted eigenvalue estimates $\hat{\lambda}_i$ are given as $\hat{\lambda}_i = \lambda_i - \frac{1}{M_r(L+1)-M_t}\sum_{j=M_t+1}^{(L+1)M_r}\lambda_j$ for $1 \leqslant i \leqslant M_t$. Thus, the estimated MIMO channel $\tilde{\mathbf{H}}$ with noise reduction is obtained as

$$\tilde{\mathbf{H}} = \mathbf{U}[:, 1 : M_t]\text{diag}[\sqrt{\hat{\lambda}_1}\ \sqrt{\hat{\lambda}_2}\ ...\ \sqrt{\hat{\lambda}_{M_t}}]\mathbf{V}^\dagger\ . \tag{3.18}$$

The channel ambiguity matrix $\mathbf{V}$ can be estimate by

$$\begin{aligned}\hat{\mathbf{V}} &= \arg\min_{\mathbf{V}\mathbf{V}^\dagger=\mathbf{I}_{\mathbf{M_t}}} ||\tilde{\mathbf{H}} - \mathbf{H}\mathbf{V}||_F^2 \\ &= \arg\max_{\mathbf{V}\mathbf{V}^\dagger=\mathbf{I}_{\mathbf{M_t}}} \text{tr}(\mathbf{V}^\dagger\mathbf{H}^\dagger\tilde{\mathbf{H}})\ .\end{aligned} \tag{3.19}$$

When we use the singular value decomposition (SVD) to decompose $\mathbf{H}^\dagger\tilde{\mathbf{H}}$ into $\mathbf{R}\mathbf{Q}\mathbf{W}^\dagger$, the estimated channel ambiguity matrix is given as $\hat{\mathbf{V}} = \mathbf{R}\mathbf{W}^\dagger$. Thus, the estimated MIMO channel $\mathbf{H}$ is obtained as

$$\hat{\mathbf{H}} = \tilde{\mathbf{H}}\hat{\mathbf{V}}\ . \tag{3.20}$$

But from the simulation, we find that noise reduction can not help too much for the channel estimation performance when the SNR is at intermediate and high regimes. It means that we can directly obtain the estimated MIMO channel $\hat{\mathbf{H}} = \check{\mathbf{H}}\hat{\mathbf{V}}$ without noise reduction in mid- and high SNR regimes.

## 3.2 Proposed precoding matrices for channel estimation

In [10], the parameters $\xi(m)$ and $\rho(m)$ in (3.5) are selected as

$$\begin{cases} \xi(m) = (N+P)(1-\alpha)+\alpha, & \text{if } m = n_0, \\ \xi(m) = \alpha, & \text{if } m \neq n_0 \\ \rho(m) = \pm\delta, & \text{if } m = 0, ..., N/2-1 \end{cases} \tag{3.21}$$

where $n_0$ is an integer satisfying $0 \leq n_0 \leq N-P-1$, and $\delta < \alpha$. We know that the matrix $\mathbf{\Omega} = \mathbf{T}\mathbf{T}^\dagger$ is positive semidefinite, and to guarantee the recovery of transmitted symbols at the receiver, the matrix $\mathbf{\Omega}$ should be positive definite [10]. This imposes the constraint $\xi(m) \geq \alpha > 0$ on $\xi(m)$ , and needs $\delta < \min_{0 \leq m < N} \ \xi(m)$ , where $\delta = \max_{0 \leq m < N/2} \ |\rho(m)|$. In addition, the received autocorrelation matrix $\mathbf{R_{rr}}$ was assumed to be (3.4), and the matrix $\mathbf{R_{rr}}$ is only corrupted by the noise. The precoder was derived based on minimizing the impact of unknown additive noise in [10], but the reality is that we should collect the received symbol blocks, and then, estimate the autocorrelation matrix $\mathbf{R_{rr}}$ by time average. Let us define $\mathbf{D}$=[$\mathbf{d}(0), \mathbf{d}(1) \ldots \mathbf{d}(Q-1)$], $\mathbf{R_{DD}} = \frac{\mathbf{D}\mathbf{D}^\dagger}{Q}$, $\mathbf{E}$=[$\boldsymbol{\eta}(0)$ , $\boldsymbol{\eta}(1) \ldots \boldsymbol{\eta}(Q-1)$ ], and $\mathbf{R}$ = [$\mathbf{r}(0)$ , $\mathbf{r}(1) \ldots \mathbf{r}(Q-1)$ ], where $Q$ is the number of symbol blocks for channel estimation. It can be readily shown that $\mathbf{R} = \mathcal{H}(\mathbf{T} \otimes \mathbf{I}_{M_t})\mathbf{D} + \mathbf{E}$. Further, let us denote $\boldsymbol{\gamma}$ = $\mathbf{R_{DD}} - \mathbf{I}_{NM_t}$. In [10], $\mathbf{R_{DD}}$ was assumed to be $\mathbf{I}_{NM_t}$, but this is in general not true as long as $Q$ is a finite integer. The difference between $\mathbf{R_{DD}}$ and $\mathbf{I}_{NM_t}$ turns out to be critical to the selection of precoder that leads to optimal channel estimation performance. The estimate $\mathbf{R_{rr}}$ can be written as

$$\begin{aligned} \hat{\mathbf{R}}_{\mathbf{rr}} &= \sum_{n=0}^{Q-1} \mathbf{r}(n)\mathbf{r}(n)^\dagger / Q \\ &= \mathbf{R}\mathbf{R}^\dagger / Q \\ &= (\mathcal{H}(\mathbf{T} \otimes \mathbf{I}_{M_t})\mathbf{D} + \mathbf{E})(\mathcal{H}(\mathbf{T} \otimes \mathbf{I}_{M_t})\mathbf{D} + \mathbf{E})^\dagger / Q \\ &= \mathcal{H}(\mathbf{T} \otimes \mathbf{I}_{M_t})(\mathbf{T}^\dagger \otimes \mathbf{I}_{M_t})\mathcal{H}^\dagger + \mathcal{H}(\mathbf{T} \otimes \mathbf{I}_{M_t})\boldsymbol{\gamma}(\mathbf{T}^\dagger \otimes \mathbf{I}_{M_t})\mathcal{H}^\dagger \\ &\quad + \mathcal{H}(\mathbf{T} \otimes \mathbf{I}_{M_t})\mathbf{D}\mathbf{E}^\dagger / Q + \mathbf{E}\mathbf{D}^\dagger(\mathbf{T}^\dagger \otimes \mathbf{I}_{M_t})\mathcal{H}^\dagger / Q + \mathbf{E}\mathbf{E}^\dagger / Q. \end{aligned} \tag{3.22}$$

We defined $\mathbf{\Gamma}$, $\mathbf{Z}$, and $\mathbf{\Phi}$ as

$$\begin{aligned} \mathbf{\Gamma} &\triangleq \mathcal{H}(\mathbf{T} \otimes \mathbf{I}_{M_t})\boldsymbol{\gamma}(\mathbf{T}^\dagger \otimes \mathbf{I}_{M_t})\mathcal{H}^\dagger \\ \mathbf{Z} &\triangleq \mathbf{E}\mathbf{E}^\dagger / Q \\ \mathbf{\Phi} &\triangleq \mathcal{H}(\mathbf{T} \otimes \mathbf{I}_{M_t})\mathbf{D}\mathbf{E}^\dagger / Q. \end{aligned} \tag{3.23}$$

Thus, the matrix $\hat{\mathbf{R}}_{\mathbf{rr}}$ in (3.22) can be written as

$$\begin{aligned}\hat{\mathbf{R}}_{\mathbf{rr}} &= \mathcal{H}(\mathbf{T}\otimes\mathbf{I}_{M_t})(\mathbf{T}^\dagger\otimes\mathbf{I}_{M_t})\mathcal{H}^\dagger+\mathbf{\Gamma}+\mathbf{\Phi}+\mathbf{\Phi}^\dagger+\mathbf{Z}\\ &= \mathcal{H}(\mathbf{\Omega}\otimes\mathbf{I}_{M_t})\mathcal{H}^\dagger+\mathbf{\Gamma}+\mathbf{\Phi}+\mathbf{\Phi}^\dagger+\mathbf{Z}\\ &= \sum_{i=0}^{L}\sum_{j=0}^{L}\mathbf{\Pi}^i\mathbf{\Omega}(\mathbf{\Pi}^T)^j\otimes\mathbf{H}(i)\mathbf{H}(j)^\dagger+\mathbf{\Gamma}+\mathbf{\Phi}+\mathbf{\Phi}^\dagger+\mathbf{Z}. \qquad (3.24)\end{aligned}$$

Note that in [10], $\mathbf{\Gamma}$ and $\mathbf{\Phi}$ are assumed to be $\mathbf{0}$ and $\mathbf{Z}$ is assumed to be $\mathbf{I}_{NM_r}$. If the matrix $\mathbf{\Omega}=\mathbf{T}\mathbf{T}^\dagger$ is properly designed, the matrices $\mathbf{H}(i)\mathbf{H}(j)^\dagger$ can be obtained from $\hat{\mathbf{R}}_{\mathbf{rr}}$, but the matrices $\mathbf{\Gamma}$,$\mathbf{\Phi}$,$\mathbf{\Phi}^\dagger$, and $\mathbf{Z}$, as will be shown later in the chapter 4 and 5, will affect the accuracy of $\mathbf{H}(i)\mathbf{H}(j)^\dagger$ when we get the matrices $\mathbf{H}(i)\mathbf{H}(j)^\dagger$ from $\hat{\mathbf{R}}_{\mathbf{rr}}$. In the reality, we think the matrix $\hat{\mathbf{R}}_{\mathbf{rr}}$ in (3.24) is more appropriate than $\mathbf{R}_{\mathbf{rr}}$ in (3.4) to describe the received autocorrelation matrix since the number of symbol blocks $Q$ is a finite value, and we never have the chance to get the matrix $\mathbf{R}_{\mathbf{rr}}$ in real situation. Since the parameter $Q$ has a finite value, the matrix $\mathbf{\Gamma}$ in (3.24) can not be the zero matrix. Further, the matrix $\mathbf{\Gamma}$ will always affects the channel MSE performance no matter the SNR how large is.

In this thesis, we proposed a new class of precoders, and it can be obtained by setting the parameters $\xi(m)$ and $\rho(m)$ in (3.5) as

$$\begin{cases}\xi(m)=((N+P)(1-\alpha)+\alpha)/2+\alpha/2, & \text{if } m=n_0,\\ \xi(m)=((N+P)(1-\alpha)+\alpha)/2+\alpha/2, & \text{if } m=n_0+N/2,\\ \xi(m)=\alpha, & \text{if } m\neq n_0, m\neq n_0+N/2,\\ \rho(m)=\delta, & \text{if } m=0,...,N/2-1\end{cases} \qquad (3.25)$$

where $n_0$ is an integer satisfying $0\leq n_0\leq N/2-1$, and $\delta<\alpha$. As will be shown numerically in chapter 5, the channel estimator using the proposed precoder can reduce the channel estimation error, compared with the channel estimator using the precoder in [10]. In addition, the simulation results show that the channel estimator using the proposed precoder can get better channel estimation than the channel estimator using the precoder in [10]. In the next chapter, we will study how the matrices $\mathbf{\Gamma}$,$\mathbf{\Phi}$, and $\mathbf{Z}$ would impact on the channel estimation performance.

# Chapter 4

# Analysis of the channel estimation performance

In this chapter, we analyze the channel estimation algorithm and study the relationship between the approximated autocorrelation matrix and the channel estimation performance. In the analysis, we will use a metric namely the channel-product mean square error (CPMSE), that is closely related to the channel estimation performance. Then we introduce some factors, involving data and noise statistics, that directly affect CPMSE. The impact of these factors on the channel estimation performance is finally described.

## 4.1 The channel estimation algorithm analysis based on approximated autocorrelation matrix

In this section, we will discuss the blind channel estimation algorithm when the autocorrelation matrix $\hat{\mathbf{R}_{\mathbf{rr}}}$ in (3.24) is used. In addition, we define the following operation that will be used in the derivation. For any $NM_r \times NM_r$ matrix $\mathbf{A} = [\mathbf{A}_{k,l}]$ for $0 \leq k, l \leq N-1$, where $\mathbf{A}_{k,l}$ is a block matrix of dimension $M_r \times M_r$ , define $\mathbf{\Lambda}_j(\mathbf{A}) = [\mathbf{A}_{0,j}^T \ \mathbf{A}_{1,j+1}^T \ ... \ \mathbf{A}_{N-1-j,N-1}^T]^T$ for $0 \leq j \leq N-1$, i.e., $\mathbf{\Lambda}_j(\mathbf{A})$ is the matrix formed from the $j$th block superdiagonal of $\mathbf{A}$.

To obtain the channel-product matrices $\mathbf{HH}^\dagger$ from the autocorrelation matrix $\hat{\mathbf{R}_{\mathbf{rr}}}$ in (3.24). We can express $[\mathbf{\Lambda}_{N/2}(\hat{\mathbf{R}}_{\mathbf{rr}})^T \mathbf{\Lambda}_{-N/2}(\hat{\mathbf{R}}_{\mathbf{rr}})^T \mathbf{\Lambda}_0(\hat{\mathbf{R}}_{\mathbf{rr}})^T]^T$ and
$[\mathbf{\Lambda}_{N/2+i}(\hat{\mathbf{R}}_{\mathbf{rr}})^T \mathbf{\Lambda}_{-N/2+i}(\hat{\mathbf{R}}_{\mathbf{rr}})^T \mathbf{\Lambda}_i(\hat{\mathbf{R}}_{\mathbf{rr}})^T \mathbf{\Lambda}_{-N+i}(\hat{\mathbf{R}}_{\mathbf{rr}})^T]^T$ as, respectively

$$[\mathbf{\Lambda}_{N/2}(\hat{\mathbf{R}}_{\mathbf{rr}})^T\mathbf{\Lambda}_{-N/2}(\hat{\mathbf{R}}_{\mathbf{rr}})^T\mathbf{\Lambda}_0(\hat{\mathbf{R}}_{\mathbf{rr}})^T]^T = ([\mathbf{A}_0^T\ \mathbf{A}_0^T\ \mathbf{B}_0^T]^T \otimes \mathbf{I}_{M_r})\mathbf{\Lambda}_0(\mathbf{H}\mathbf{H}^\dagger)$$
$$+[\mathbf{\Lambda}_{N/2}(\mathbf{\Gamma})^T\mathbf{\Lambda}_{-N/2}(\mathbf{\Gamma})^T\mathbf{\Lambda}_0(\mathbf{\Gamma})^T]^T + [\mathbf{\Lambda}_{N/2}(\mathbf{\Phi})^T\mathbf{\Lambda}_{-N/2}(\mathbf{\Phi})^T\mathbf{\Lambda}_0(\mathbf{\Phi})^T]^T$$
$$+[\mathbf{\Lambda}_{N/2}(\mathbf{\Phi}^\dagger)^T\mathbf{\Lambda}_{-N/2}(\mathbf{\Phi}^\dagger)^T\mathbf{\Lambda}_0(\mathbf{\Phi}^\dagger)^T]^T + [\mathbf{\Lambda}_{N/2}(\mathbf{Z})^T\mathbf{\Lambda}_{-N/2}(\mathbf{Z})^T\mathbf{\Lambda}_0(\mathbf{Z})^T]^T \qquad (4.1)$$

$$\begin{aligned}
& [\mathbf{\Lambda}_{N/2+i}(\hat{\mathbf{R}}_{\mathbf{rr}})^T\mathbf{\Lambda}_{-N/2+i}(\hat{\mathbf{R}}_{\mathbf{rr}})^T\mathbf{\Lambda}_i(\hat{\mathbf{R}}_{\mathbf{rr}})^T\mathbf{\Lambda}_{-N+i}(\hat{\mathbf{R}}_{\mathbf{rr}})^T]^T \\
= \quad & ([\mathbf{A}_i^T\ \mathbf{A}_i^T\ \mathbf{B}_i^T]^T \otimes \mathbf{I}_{M_r})\mathbf{\Lambda}_i(\mathbf{H}\mathbf{H}^\dagger) \\
& +[\mathbf{\Lambda}_{N/2+i}(\mathbf{\Gamma})^T\mathbf{\Lambda}_{-N/2+i}(\mathbf{\Gamma})^T\mathbf{\Lambda}_i(\mathbf{\Gamma})^T\mathbf{\Lambda}_{-N+i}(\mathbf{\Gamma})^T]^T \\
& +[\mathbf{\Lambda}_{N/2+i}(\mathbf{\Phi})^T\mathbf{\Lambda}_{-N/2+i}(\mathbf{\Phi})^T\mathbf{\Lambda}_i(\mathbf{\Phi})^T\mathbf{\Lambda}_{-N+i}(\mathbf{\Phi})^T]^T \\
& +[\mathbf{\Lambda}_{N/2+i}(\mathbf{\Phi}^\dagger)^T\mathbf{\Lambda}_{-N/2+i}(\mathbf{\Phi}^\dagger)^T\mathbf{\Lambda}_i(\mathbf{\Phi}^\dagger)^T\mathbf{\Lambda}_{-N+i}(\mathbf{\Phi}^\dagger)^T]^T \\
& +[\mathbf{\Lambda}_{N/2+i}(\mathbf{Z})^T\mathbf{\Lambda}_{-N/2+i}(\mathbf{Z})^T\mathbf{\Lambda}_i(\mathbf{Z})^T\mathbf{\Lambda}_{-N+i}(\mathbf{Z})^T]^T, \text{for } 1 \le i \le L. \qquad (4.2)
\end{aligned}$$

In (4.1) and (4.2), the $N/2 \times (L-i+1)$ matrix $\mathbf{A}_i$ for $0 \le i \le L$ and the $N \times (L-i+1)$ matrix $\mathbf{B}_i$ for $0 \le i \le L$ are defined in (3.11) and (3.12), respectively. In addition, the matrices $\mathbf{\Gamma}$, $\mathbf{Z}$, $\mathbf{\Phi}$ are defined in (3.23). Let $\mathbf{C}_i$ be the pseudoinverse matrix of $[\mathbf{A}_i^T\ \mathbf{A}_i^T\ \mathbf{B}_i^T]^T \otimes \mathbf{I}_{M_r}$. So, $\mathbf{C}_i$ can be given as (3.13). In addition, let us denote

$$\begin{aligned}
\mathbf{\Gamma}_0 &= [\mathbf{\Lambda}_{N/2}(\mathbf{\Gamma})^T\mathbf{\Lambda}_{-N/2}(\mathbf{\Gamma})^T\mathbf{\Lambda}_0(\mathbf{\Gamma})^T]^T \\
\mathbf{\Phi}_0 &= [\mathbf{\Lambda}_{N/2}(\mathbf{\Phi})^T\mathbf{\Lambda}_{-N/2}(\mathbf{\Phi})^T\mathbf{\Lambda}_0(\mathbf{\Phi})^T]^T \\
\Psi_0 &= [\mathbf{\Lambda}_{N/2}(\mathbf{\Phi}^\dagger)^T\mathbf{\Lambda}_{-N/2}(\mathbf{\Phi}^\dagger)^T\mathbf{\Lambda}_0(\mathbf{\Phi}^\dagger)^T]^T \\
\mathbf{Z}_0 &= [\mathbf{\Lambda}_{N/2}(\mathbf{Z})^T\mathbf{\Lambda}_{-N/2}(\mathbf{Z})^T\mathbf{\Lambda}_0(\mathbf{Z})^T]^T. \qquad (4.3)
\end{aligned}$$

Besides, for $1 \le i \le L$, define

$$\begin{aligned}
\mathbf{\Gamma}_i &= [\mathbf{\Lambda}_{N/2+i}(\mathbf{\Gamma})^T\mathbf{\Lambda}_{-N/2+i}(\mathbf{\Gamma})^T\mathbf{\Lambda}_i(\mathbf{\Gamma})^T\mathbf{\Lambda}_{-N+i}(\mathbf{\Gamma})^T]^T \\
\mathbf{\Phi}_i &= [\mathbf{\Lambda}_{N/2+i}(\mathbf{\Phi})^T\mathbf{\Lambda}_{-N/2+i}(\mathbf{\Phi})^T\mathbf{\Lambda}_i(\mathbf{\Phi})^T\mathbf{\Lambda}_{-N+i}(\mathbf{\Phi})^T]^T \\
\Psi_i &= [\mathbf{\Lambda}_{N/2+i}(\mathbf{\Phi}^\dagger)^T\mathbf{\Lambda}_{-N/2+i}(\mathbf{\Phi}^\dagger)^T\mathbf{\Lambda}_i(\mathbf{\Phi}^\dagger)^T\mathbf{\Lambda}_{-N+i}(\mathbf{\Phi}^\dagger)^T]^T \\
\mathbf{Z}_i &= [\mathbf{\Lambda}_{N/2+i}(\mathbf{Z})^T\mathbf{\Lambda}_{-N/2+i}(\mathbf{Z})^T\mathbf{\Lambda}_i(\mathbf{Z})^T\mathbf{\Lambda}_{-N+i}(\mathbf{Z})^T]^T. \qquad (4.4)
\end{aligned}$$

Then, the estimate of $\mathbf{\Lambda}_i(\mathbf{H}\mathbf{H}^\dagger)$ are obtained as, respectively

$$\mathbf{\Lambda}_0(\tilde{\mathbf{H}}\tilde{\mathbf{H}}^\dagger) \quad = \quad \mathbf{C}_0[\mathbf{\Lambda}_{N/2}(\hat{\mathbf{R}}_{\mathbf{rr}})^T\mathbf{\Lambda}_{-N/2}(\hat{\mathbf{R}}_{\mathbf{rr}})^T\mathbf{\Lambda}_0(\hat{\mathbf{R}}_{\mathbf{rr}})^T]^T$$

$$= \quad \mathbf{\Lambda}_0(\mathbf{H}\mathbf{H}^\dagger) + \mathbf{C}_0(\mathbf{\Gamma}_0 + \mathbf{\Phi}_0 + \Psi_0 + \mathbf{Z}_0). \tag{4.5}$$

$$\begin{aligned} \mathbf{\Lambda}_i(\tilde{\mathbf{H}}\tilde{\mathbf{H}}^\dagger) &= \mathbf{C}_i[\mathbf{\Lambda}_{N/2+i}(\hat{\mathbf{R}}_{\mathbf{rr}})^T\mathbf{\Lambda}_{-N/2+i}(\hat{\mathbf{R}}_{\mathbf{rr}})^T\mathbf{\Lambda}_i(\hat{\mathbf{R}}_{\mathbf{rr}})^T\mathbf{\Lambda}_{-N+i}(\hat{\mathbf{R}}_{\mathbf{rr}})^T]^T \\ &= \mathbf{\Lambda}_i(\mathbf{H}\mathbf{H}^\dagger) + \mathbf{C}_i(\mathbf{\Gamma}_i + \mathbf{\Phi}_i + \Psi_i + \mathbf{Z}_i), \text{for } i = 1 \ldots L. \end{aligned} \tag{4.6}$$

If the second term of (4.5) and (4.6) are equal to the zero matrix, $\mathbf{\Lambda}_i(\mathbf{H}\mathbf{H}^\dagger)$ for $i = 0, 1, ..., L$ are precisely obtained. However, since $\mathbf{C}_0$ and $\mathbf{C}_i$ must not be the zero matrix, we need the second term of (4.5) and (4.6) as close to a zero matrix as possible. Using $\mathbf{\Lambda}_i(\tilde{\mathbf{H}}\tilde{\mathbf{H}}^\dagger)$, $0 \leqslant i \leqslant L$, we can construct the matrix $\tilde{\mathbf{H}}\tilde{\mathbf{H}}^\dagger$. Then, we can decompose $\tilde{\mathbf{H}}\tilde{\mathbf{H}}^\dagger$ by the eigenvalue decomposition, and the MIMO channel estimation are obtained by removing the effect of ambiguity matrix as given in (3.20). As will be shown later in Section 4.3, the accuracy of the channel-product matrices $\tilde{\mathbf{H}}\tilde{\mathbf{H}}^\dagger$ (estimated from $\hat{\mathbf{R}}_{\mathbf{rr}}$ ) has a strong effect on the channel estimation MSE. In the next section, we first study the factors that affect CPMSE.

## 4.2 The factors that affect CPMSE

In this section, we want to analyze the factors which are correlated to channel-product mean square error (CPMSE). Since $\mathbf{\Lambda}_{-i}(\tilde{\mathbf{H}}\tilde{\mathbf{H}}^\dagger) - \mathbf{\Lambda}_{-i}(\mathbf{H}\mathbf{H}^\dagger) = (\mathbf{\Lambda}_i(\tilde{\mathbf{H}}\tilde{\mathbf{H}}^\dagger) - \mathbf{\Lambda}_i(\mathbf{H}\mathbf{H}^\dagger))^\dagger$, we can get

$$||\mathbf{\Lambda}_i(\tilde{\mathbf{H}}\tilde{\mathbf{H}}^\dagger) - \mathbf{\Lambda}_i(\mathbf{H}\mathbf{H}^\dagger)||_F^2 = ||\mathbf{\Lambda}_{-i}(\tilde{\mathbf{H}}\tilde{\mathbf{H}}^\dagger) - \mathbf{\Lambda}_{-i}(\mathbf{H}\mathbf{H}^\dagger)||_F^2 \,. \tag{4.7}$$

Then, the channel-product mean square error is given by

$$\begin{aligned} &T_F \triangleq E(||(\tilde{\mathbf{H}}\tilde{\mathbf{H}}^\dagger) - (\mathbf{H}\mathbf{H}^\dagger)||_F^2) \\ &= E(||\mathbf{\Lambda}_0(\tilde{\mathbf{H}}\tilde{\mathbf{H}}^\dagger) - \mathbf{\Lambda}_0(\mathbf{H}\mathbf{H}^\dagger)||_F^2 + \sum_{i=1}^{L} ||\mathbf{\Lambda}_i(\tilde{\mathbf{H}}\tilde{\mathbf{H}}^\dagger) - \mathbf{\Lambda}_i(\mathbf{H}\mathbf{H}^\dagger)||_F^2 \\ &+ \sum_{i=1}^{L} ||\mathbf{\Lambda}_{-i}(\tilde{\mathbf{H}}\tilde{\mathbf{H}}^\dagger) - \mathbf{\Lambda}_{-i}(\mathbf{H}\mathbf{H}^\dagger)||_F^2) \\ &= E(||\mathbf{\Lambda}_0(\tilde{\mathbf{H}}\tilde{\mathbf{H}}^\dagger) - \mathbf{\Lambda}_0(\mathbf{H}\mathbf{H}^\dagger)||_F^2 + 2\sum_{i=1}^{L} ||\mathbf{\Lambda}_i(\tilde{\mathbf{H}}\tilde{\mathbf{H}}^\dagger) - \mathbf{\Lambda}_i(\mathbf{H}\mathbf{H}^\dagger)||_F^2) \\ &= E(||\mathbf{C}_0(\mathbf{\Gamma}_0 + \mathbf{\Phi}_0 + \mathbf{\Psi}_0 + \mathbf{Z}_0)||_F^2 + 2\sum_{i=1}^{L} ||\mathbf{C}_i(\mathbf{\Gamma}_i + \mathbf{\Phi}_i + \mathbf{\Psi}_i + \mathbf{Z}_i)||_F^2). \end{aligned} \tag{4.8}$$

Since the matrices $\mathbf{\Gamma}$, $\mathbf{\Phi}$, and $\mathbf{Z}$ in (3.24) affect the channel-product mean square error, and we want to analyze the term that dominates the channel-product MSE. Thus, we denote

$$\Gamma_F = E(||\mathbf{C}_0\mathbf{\Gamma}_0||_F^2 + 2\sum_{i=1}^{L}||\mathbf{C}_i\mathbf{\Gamma}_i||_F^2) \tag{4.9}$$

$$\Phi_F = E(||\mathbf{C}_0\mathbf{\Phi}_0||_F^2 + 2\sum_{i=1}^{L}||\mathbf{C}_i\mathbf{\Phi}_i||_F^2) \tag{4.10}$$

$$\Psi_F = E(||\mathbf{C}_0\mathbf{\Psi}_0||_F^2 + 2\sum_{i=1}^{L}||\mathbf{C}_i\mathbf{\Psi}_i||_F^2) \tag{4.11}$$

$$Z_F = E(||\mathbf{C}_0\mathbf{Z}_0||_F^2 + 2\sum_{i=1}^{L}||\mathbf{C}_i\mathbf{Z}_i||_F^2). \tag{4.12}$$

We define $G_F \triangleq \Gamma_F + \Phi_F + \Psi_F + Z_F$, and it can be shown that

$$E(||(\tilde{\mathbf{H}}\tilde{\mathbf{H}}^\dagger) - (\mathbf{H}\mathbf{H}^\dagger)||_F^2) = G_F. \tag{4.13}$$

The steps of the proof is given in the appendix. Moreover, we called $\Gamma_F$, $\Phi_F$, $\Psi_F$, and $Z_F$, the error caused by the difference between $\mathbf{R_{DD}}$(i.e., $\mathbf{D}\mathbf{D}^\dagger/Q$) and the identity matrix, the error caused by the difference between $\mathbf{R_{DE}}$(i.e., $\mathbf{D}\mathbf{E}^\dagger/Q$) and the zero matrix, the error caused by the difference between $\mathbf{R_{ED}}$(i.e., $\mathbf{E}\mathbf{D}^\dagger/Q$) and the zero matrix, and the error caused by the noise term (i.e., $\mathbf{E}\mathbf{E}^\dagger/Q$), respectively. In this section, we know that the CPMSE equals to the sum of the error factors. In addition, as will be shown later in Chapter 5, instead of the error factor $Z_F$, the error factor $\Gamma_F$ play an important role for channel estimation performance when the SNR is larger than $0$ dB. In next section, we will show that the CPMSE is highly related to the channel estimation MSE.

## 4.3 The relationship between the CPMSE and the channel MSE

In this section, we want to learn the relation between the CPMSE and the channel MSE. The CPMSE is defined in (4.9), and the channel MSE is given by

$$E(||\hat{\mathbf{H}} - \mathbf{H})||)_F^2. \tag{4.14}$$

If we let $\hat{\mathbf{H}} = \mathbf{H} + \Delta\mathbf{H}$, the CPMSE can be expressed as

$$E(||(\tilde{\mathbf{H}}\tilde{\mathbf{H}}^\dagger - \mathbf{H}\mathbf{H}^\dagger||)_F^2$$

$$= E(||\hat{\mathbf{H}}\hat{\mathbf{H}}^{\dagger} - \mathbf{H}\mathbf{H}^{\dagger}||)_F^2$$
$$= E(||(\Delta\mathbf{H})\mathbf{H}^{\dagger} + \mathbf{H}(\Delta\mathbf{H})^{\dagger} + (\Delta\mathbf{H})(\Delta\mathbf{H})^{\dagger}||)_F^2.$$

We note the channel MSE in $(4.14)$ can be written as $E(||\Delta\mathbf{H}||)_F^2$. The smaller the CPMSE we have, the smaller $\Delta\mathbf{H}$ we obtain. The smaller $\Delta\mathbf{H}$ we get, the smaller channel MSE we have. In summary, we showed that the matrices $\mathbf{\Gamma}$, $\mathbf{\Phi}$, and $\mathbf{Z}$ in (3.24) affect the CPMSE. Besides, we revealed four error factors ($\Gamma_F$, $\Phi_F$, $\Psi_F$, $Z_F$) that can be indicators for the channel estimation performance. In the next chapter, We will give some simulation examples to demonstrate the importance of the error factor $\Gamma_F$. Further, we will use the error factors and the CPMSE to explain why the proposed precoder has a better channel estimation performance.

# Chapter 5

# Simulation Results

This chapter presents six simulation examples to analyze the channel estimation MSE of the channel estimation algorithm, using the proposed precoder and the precoder in [10], which is marked with "Shin," and the channel estimator in [3] which is marked with "Chen." In the following simulations, we consider an MIMO blocks transmission system with a CP, equipped with two transmit($M_t = 2$) and two receive antennas($M_r = 2$). The number of subcarriers is $N = 16$, the MIMO channel order is $L = 3$, and the length of the CP is $P = 3$. The precoding matrix is $\mathbf{T} = \mathbf{\Omega}^{1/2}$.

We use 16-QAM to generate the information symbols $d_i(n, k)$'s, and let the signal power $\sigma_d^2 = 1$. The perturbed noise at each receive antenna is an additive complex white Gaussian noise with zero mean and variance $\sigma_\eta^2$. The SNR is defined as $\sigma_d^2/\sigma_\eta^2 = 1/\sigma_\eta^2$. In other words, $\sigma_\eta^2$ can be obtained as 1/SNR. Entries of each channel tap $\mathbf{H}(l)$ are independent and identically distributed(i.i.d), and are randomly generated from a $\mathcal{CN}(0, 1/(L+1))$ with a uniform power delay profile. One thousand independent realizations of the channel matrix $\mathcal{H}$ ($N_m = 1000$) are used for channel estimation. The channel-product mean square error (CPMSE) and the channel mean square error (MSE) are given as

$$\text{CPMSE} \triangleq \frac{1}{N_m}\sum_{k=1}^{N_m} ||(\tilde{\mathbf{H}}_{(k)}\tilde{\mathbf{H}}_{(k)}^{\dagger}) - (\mathbf{H}_{(k)}\mathbf{H}_{(k)}^{\dagger})||_F^2$$

$$\text{MSE} \triangleq \frac{1}{N_m M_t M_r (L+1)}\sum_{k=1}^{N_m} ||\mathbf{H}_{(k)} - \hat{\mathbf{H}}_{(k)}||_F^2 \,. \tag{5.1}$$

Simulation Example 1: In this example, we consider the channel estimate MSE of the channel estimator with and without noise reduction which was mentioned in Section 3.1. The coefficients of the proposed precoder are chosen based on (3.25) with $\alpha = 0.1$ and $\delta = 0$. The coefficients of Shin's and Chen's precoders are chosen based on (3.21) with $\alpha = 0.1$ and $\delta = 0$. The simulation result is shown in Fig. 5.1. We can see that

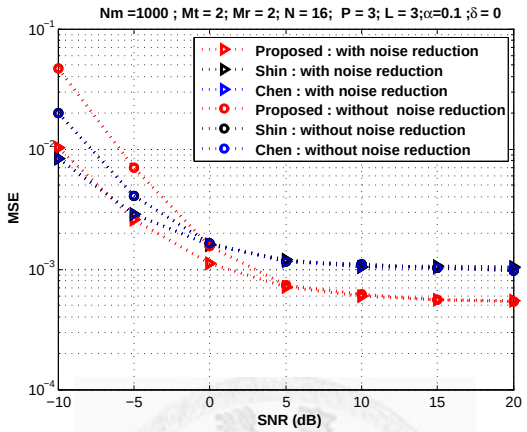


(a)

Figure 5.1: Comparison of MSE performance when the channel estimator with the noise reduction and without noise reduction.

the channel estimation performance of the channel estimator using the proposed precoder with those of the channel estimator using the precoders of "Shin" and "Chen" are very close in mid- and high SNR regimes. It suggests noise reduction does not help too much in mid- and high SNR regimes. Thus, in mid- and high SNR regimes, we can reduce the complexity of the channel estimation algorithm by estimating the channel coefficients without noise reduction.

Simulation Example 2: We want to learn the channel estimation MSE performance according to different values of SNR. The coefficients of the proposed precoder are chosen based on (3.25) with $\alpha = 0.1$ and $\delta = 0$. The coefficients of Shin's and Chen's precoders are chosen based on (3.21) with $\alpha = 0.1$ and $\delta = 0$.

The simulation result is shown in Fig. 5.2. In this example, we found that even when the noise is absent, the MSE performance is nonzero since the matrix $\mathbf{\Gamma}$ defined in (3.23) is nonzero. In addition, significant improvement of MSE performance is seen only when the SNR increases from a low SNR regime to an intermediate one. In [10], they proposed the procoder that is optimized in the sense of minimizing the impact of unknown additive

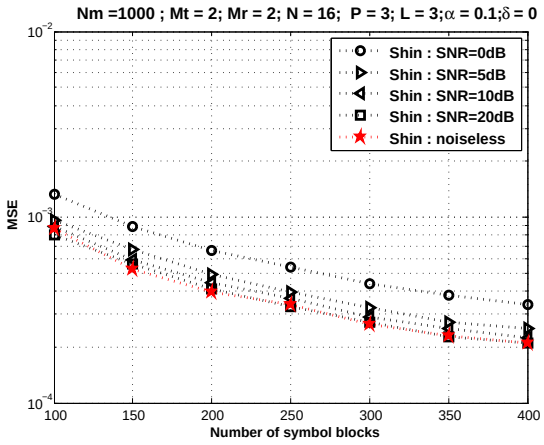


(a)

Figure 5.2: Comparison of MSE performances according to different value of SNR.

noise. However, we observed that the noise is not a crucial role for channel estimation MSE in mid- and high SNR regimes. We therefore presume that some factor other than the noise plays a more important role for channel estimation MSE in mid- and high SNR regimes, as will be shown in details in the next simulation example.

Simulation Example 3: In this example, we compared the channel estimation performance of the channel estimator using the proposed precoder with those of the channel estimator using the precoders of "Shin" and "Chen". We consider the situation when SNR = 20 dB. The coefficients of the proposed precoder are chosen based on (3.25) with $\alpha = 0.1, 0.3, 0.7,$ and $0.9$ and with $\delta = 0$, respectively. The coefficients of Shin's and Chen's precoders are chosen based on (3.21) with $\alpha = 0.1, 0.3, 0.7,$ and $0.9$ and with $\delta = 0$, respectively. The channel estimation MSE, the channel-product MSE(CPMSE), and the error factors ($\Phi_F$,$\Psi_F$,$Z_F$,$\Gamma_F$) defined in Chapter 4 versus the number of symbol blocks are shown in Fig. 5.3. The CPMSE equals to the sum of the error factors. We expect that the CPMSE is highly related to the MSE, and the smaller CPMSE we have, the smaller MSE. As seen in Fig. 5.3, we can find that $\Gamma_F$ is much larger than other error factors. Thus, we think $\Gamma_F$ is the most crucial factor for the CPMSE performance when SNR = 20 dB. This can be seen in Fig. 5.3(e) and Fig. 5.3(f), the CPMSE is very close to the error factor $\Gamma_F$. In Fig. 5.3(e), we can see that the error factor $\Gamma_F$ of the channel estimator using the proposed precoder is much smaller than those of the channel estimator using the precoders of "Shin" and "Chen" for $\alpha < 0.7$. In Fig. 5.3(c), we find that the MSE

performance of the channel estimator using the proposed precoder is also much smaller than those of the channel estimator using the precoders of "Shin" and "Chen" for $\alpha < 0.7$. In addition, Fig. 5.3(c) shows that the channel estimation performs better for smaller $\alpha$, which is consistent with the $\Gamma_F$ values we observe in Fig. 5.3(e). Moreover, the MSE performance is consistently improved as the number of symbol blocks increases. This reflects the fact that the more reliable the autocorrelation matrix estimate of the received signal, the more accurate the channel estimate by the channel estimator [10].

Simulation Example 4: In this example, we compared the channel estimation performance of the channel estimator using the proposed precoder with those of the channel estimator using the precoders of "Shin" and "Chen". The coefficients of the proposed precoder are chosen based on (3.25) with $\alpha = 0.1, 0.3, 0.7,$ and $0.9$ and with $\delta = 0$, respectively. The coefficients of Shin's and Chen's precoders are chosen based on (3.21) with $\alpha = 0.1, 0.3, 0.7,$ and $0.9$ and with $\delta = 0$, respectively. The channel estimation MSE, the channel-product MSE(CPMSE), and the error factors ($\Phi_F$,$\Psi_F$,$Z_F$,$\Gamma_F$) defined in Chapter 4 versus SNR are shown in Fig. 5.4. The number of symbol blocks is set to 100. In Fig. 5.4(e), we observe that although the estimation performance is improved when the SNR increases from a low value to an intermediate one, the rate of the performance improvement becomes insignificant at intermediate and high SNR regimes. This can be seen in Fig. 5.4(a) with Fig. 5.4(d), where we observe that in negative SNR regime the values of $Z_F$ is larger than that of $\Gamma_F$; the error factor $Z_F$ become an important role for the MSE performance in this regime. In mid- and high SNR regimes, the values of $Z_F$ is much smaller than that of $\Gamma_F$; the error factor $\Gamma_F$ become important role for channel estimation in mid- and high SNR regimes. This is consistent with our claim that the error factor $\Gamma_F$, instead of the noise, is the crucial factor of channel estimation performance especially when the SNR is at mid- and high regimes. In addition, the channel estimator using the proposed precoder decreases the $\Gamma_F$ compared with the channel estimator using the precoders of "Shin" and "Chen" for $\alpha < 0.7$. From Fig. 5.4(e), we can see that the channel estimator using the proposed precoder has a better MSE performance than the channel estimator using the precoders of "Shin" and "Chen" when SNR is larger than 0 dB and $\alpha < 0.7$. This simulation example shows that reducing the error factor $\Gamma_F$ is more important than reducing $Z_F$ when SNR is larger than 0 dB.

Simulation Example 5: In this example, we will explore how the $\delta$ parameter defined in Section 3.1 will affect the channel estimation performance. We compare the channel estimation performance of the channel estimator using the proposed precoder with that of the channel estimator using the precoder of "Shin". The coefficients of the proposed precoder are chosen based on (3.25) with $\delta = 0, 0.3$, and $0.6$ and with $\alpha = 0.7$, respectively. The coefficients of Shin's precoder are chosen based on (3.21) with $\delta = 0, 0.3$, and $0.6$ and with $\alpha = 0.7$, respectively. We consider the situation when SNR = 20 dB. The channel estimation MSE, the channel-product MSE(CPMSE), and the error factors ($\Phi_F$,$\Psi_F$,$Z_F$,$\Gamma_F$) defined in Chapter 4 versus the number of symbol blocks are shown in Fig. 5.5. In previous examples, we show that the error factors $\Phi_F$,$\Psi_F$, and $Z_F$ are not important role for channel estimation performance when SNR = 20dB, so we will discuss the error factor $\Gamma_F$ especially. Fig. 5.5(e) presents the MSE performance as a function of the number of symbol blocks. The figure shows that regardless of the value of $\delta$, the MSE performance is almost identical with the fixed $\alpha$ when the precoder of "Shin" is used. When the proposed precoders are used, however, the MSE performance will decreases as $\delta$ decreases from 0.6 to 0. As seen in Fig. 5.5(a), we find that regardless of the value of $\delta$, the error factor $\Gamma_F$ almost identical with the fixed $\alpha$ when the channel estimator using the precoder of "Shin", but the error factor $\Gamma_F$ is decreased as $\delta$ decreased with $\alpha$ fixed when the channel estimator using the proposed precoder. Thus the choice of $\delta$ appears to play a less important role in channel estimation when the precoder of "Shin" is used, but a choice of a small value of $\delta$ leads to a better channel estimation performance when the proposed precoder is used.

Simulation Example 6: In this example, we want to learn how the different modulation schemes would impact on the channel estimation performance. We use three modulation schemes, namely, QPSK, 16-QAM, and 64-QAM to generate the information symbols $d_i(n,k)$'s. The coefficients of the proposed precoder are chosen based on (3.25) with $\delta = 0$ and $\alpha = 0.1$. The coefficients of Shin's precoder are chosen based on (3.21) with $\delta = 0$ and $\alpha = 0.1$. We consider the situation when SNR = 20 dB. The channel estimation MSE, the channel-product MSE(CPMSE), and the error factors ($\Phi_F$,$\Psi_F$,$Z_F$,$\Gamma_F$) defined in Chapter 4 versus the number of symbol blocks are shown in Fig. 5.6. In Fig. 5.6(a)-(c), we observe that the error factors $\Phi_F$,$\Psi_F$, and $Z_F$ are most identical regardless of the

modulation schemes used. In Fig. 5.6(d), we can see that the error factor $\Gamma_F$ with QPSK modulation scheme used is much smaller than that with 16-QAM used, but we can also see that the error factors $\Gamma_F$ with 64-QAM used is close to that with 16-QAM used. It suggests that using a small modulation scheme (e.g. QPSK) can result in small the error factor $\Gamma_F$ . In addition, the error factor $\Gamma_F$ is the dominant error factor for the CPMSE, and the MSE is highly related to the CPMSE. The result of Fig. 5.6(e) agrees with our expectation.

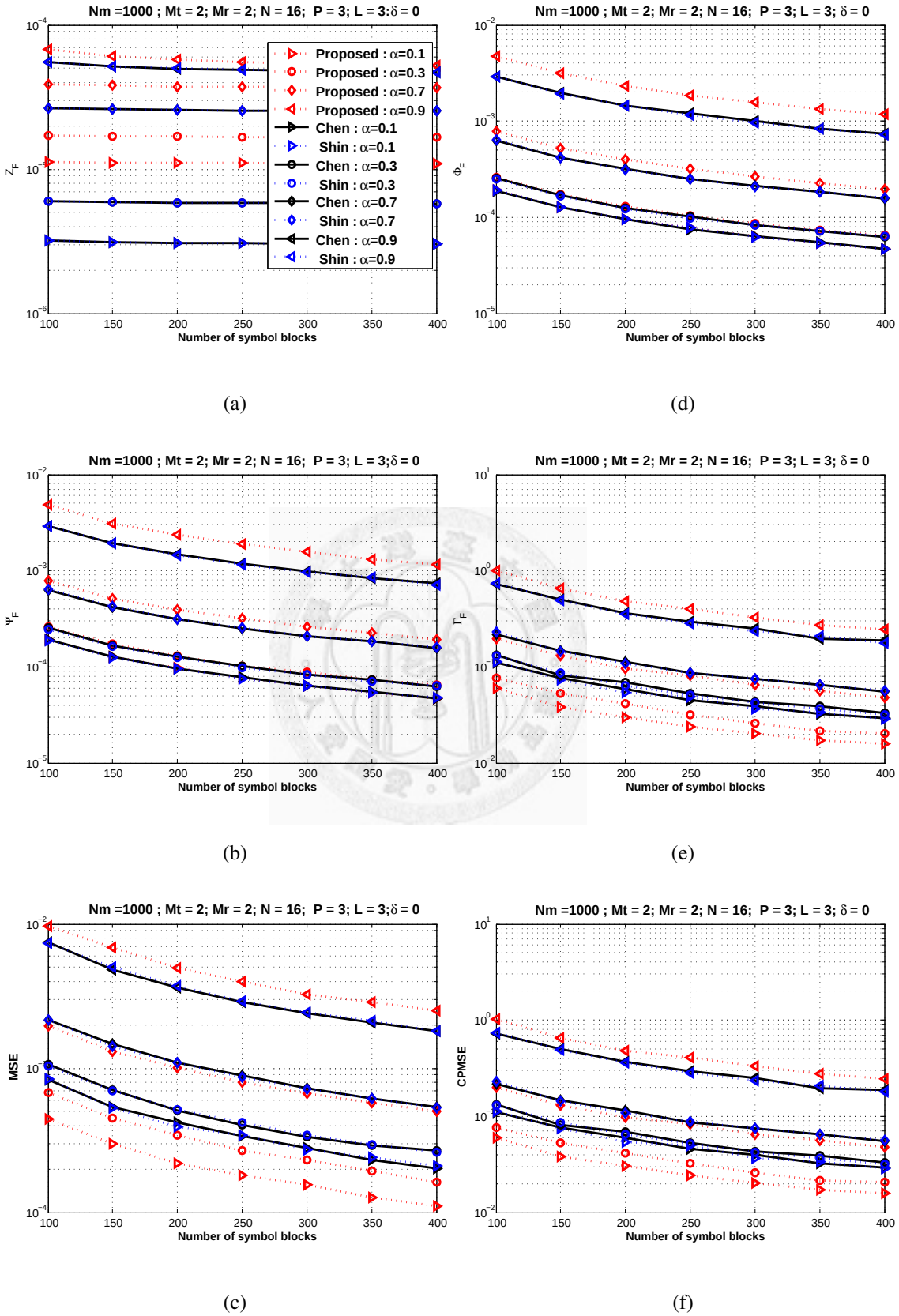


Figure 5.3: Shows the error factors, MSE, and CPMSE versus the number of symbol blocks when SNR = 20 dB. All legends are as same as Fig. 5.3(a).

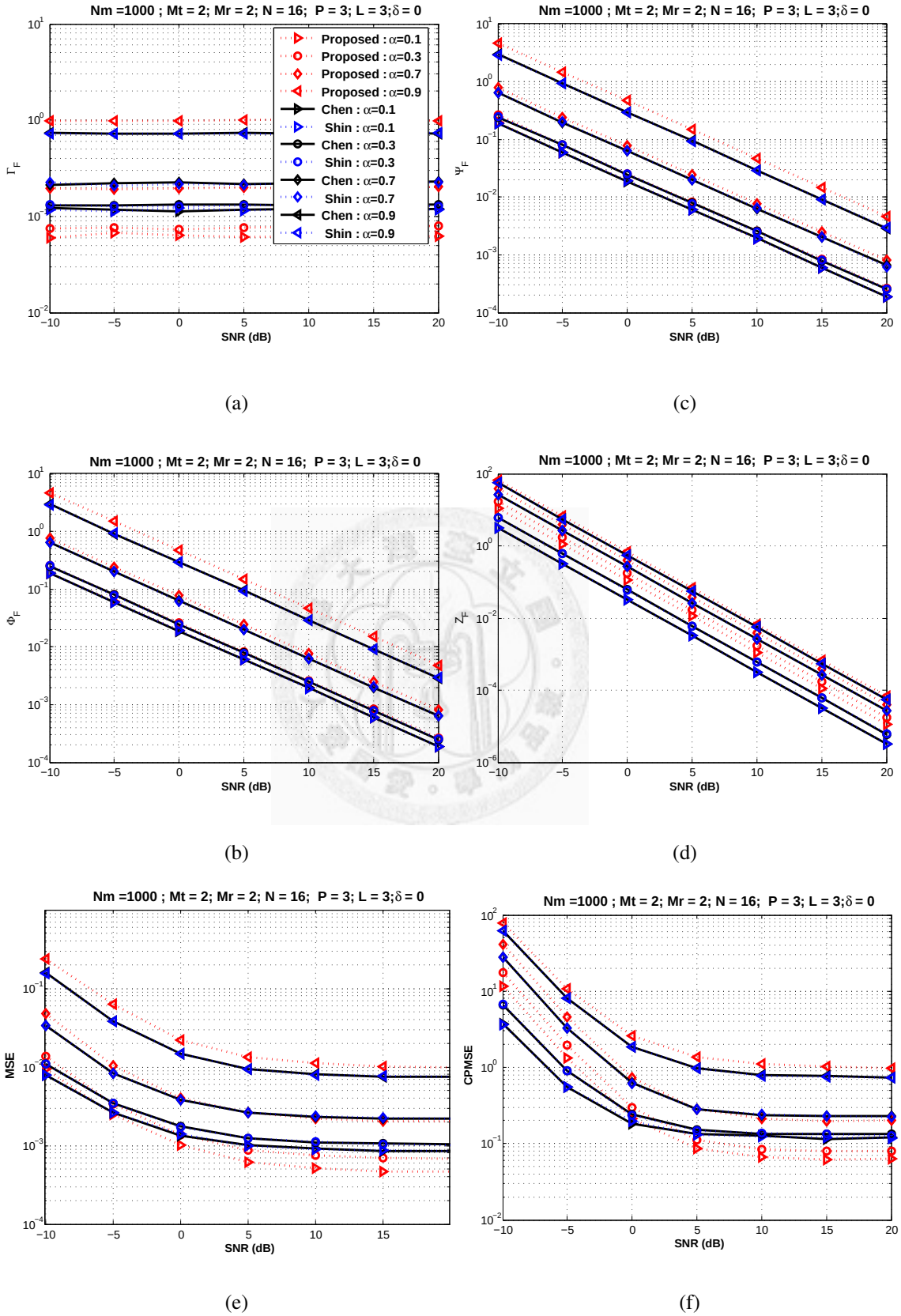


Figure 5.4: Shows the error factors, the MSE, and CPMSE versus SNR when the number of symbol blocks is equal to 100. All legends are as same as Fig. 5.4(a).

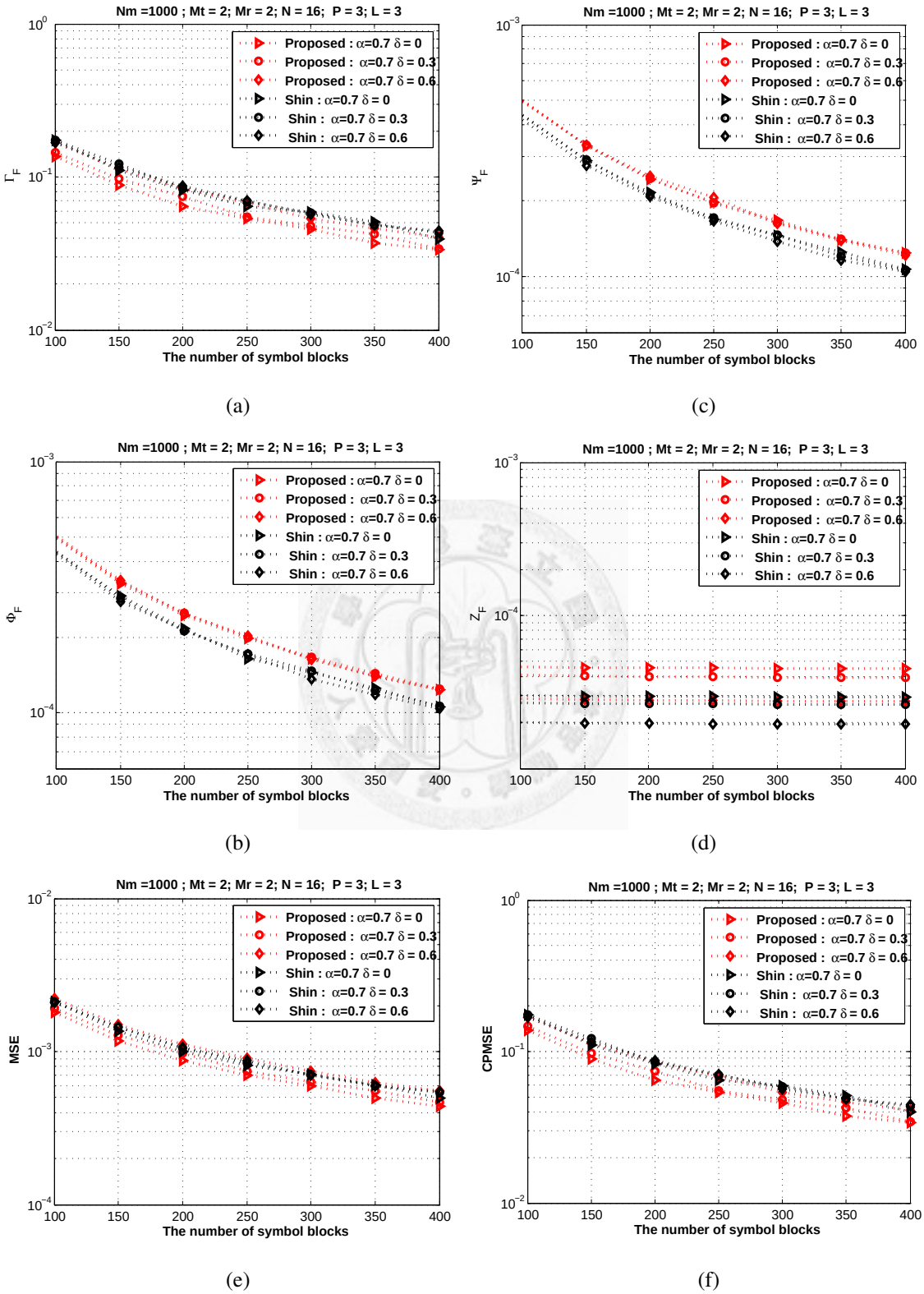


Figure 5.5: Comparison of MSE performance and the error factors according to different value of $\delta$ when $\alpha$ is fixed at 0.7 and SNR = 20 dB.

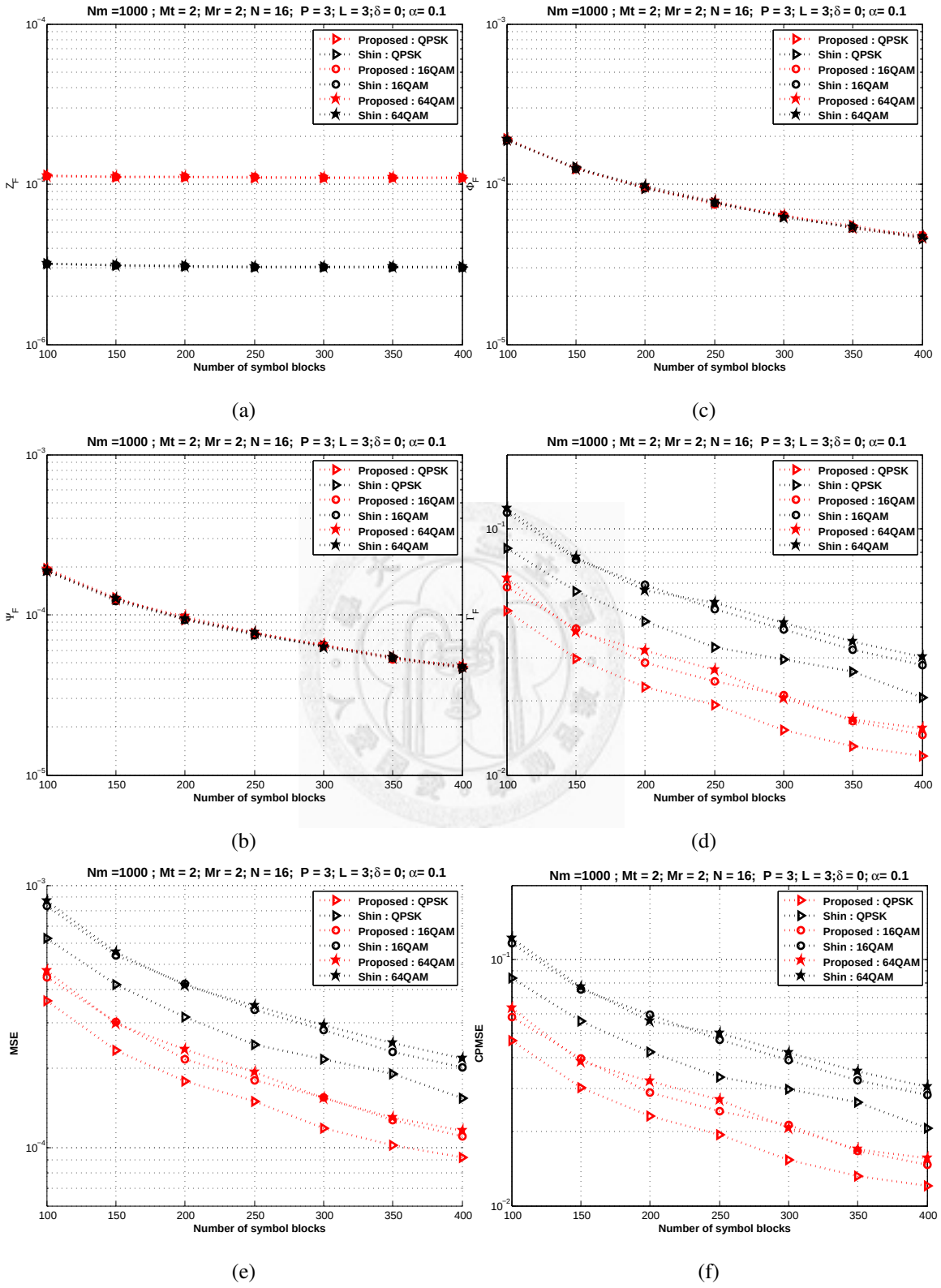


Figure 5.6: Comparison of MSE performance, the CPMSE, and the error factors according to QPSK,16-QAM, and 64-QAM when SNR = 20 dB.

# Chapter 6

# Conclusions

In this thesis, we studied the blind channel estimation problem in MIMO CP systems based on precoding at the transmitters. A new class of precoders is proposed that improves the channel estimation performance. We also introduced four error factors that are strongly related to the channel estimation performance. Simulation results show that our proposed precoders possess smaller error factors and hence justifies its performance improvement.

The simulation results show that compared with some existing precoding approaches for MIMO block transmission systems with CP, our proposed precoder obtains an accurate MIMO channel estimate as long as the number of symbol blocks is finite. In addition, we analyze the channel estimation performance according to the error factors. Furthermore, we learned how the different modulation schemes would impact on the channel estimation performance. It suggests that using a small modulation scheme can result in small the channel estimate MSE.

In the future, it is a challenging work to find an optimal precoder that considers all error factors introduced in this thesis. Another challenging work is to develop the channel estimation algorithm that has an even better performance under the same number of symbol blocks.

# Appendix A

# Appendix

In this appendix, we will show that the CPMSE equals to the sum of the error factors, and it is given in (4.13).

Proof:

$$
\begin{aligned}
&T_F = E(||\mathbf{C}_0(\mathbf{\Gamma}_0 + \mathbf{\Phi}_0 + \mathbf{\Psi}_0 + \mathbf{Z}_0)||_F^2 + 2\sum_{i=1}^{L} ||\mathbf{C}_i(\mathbf{\Gamma}_i + \mathbf{\Phi}_i + \mathbf{\Psi}_i + \mathbf{Z}_i)||_F^2) \\
&= \text{tr}(\mathbf{C}_0 E[(\mathbf{\Gamma}_0 + \mathbf{\Phi}_0 + \mathbf{\Psi}_0 + \mathbf{Z}_0)(\mathbf{\Gamma}_0^\dagger + \mathbf{\Phi}_0^\dagger + \mathbf{\Psi}_0^\dagger + \mathbf{Z}_0^\dagger)]\mathbf{C}_0^\dagger) \\
&+2\sum_{i=1}^{L} \text{tr}(\mathbf{C}_i E[(\mathbf{\Gamma}_i + \mathbf{\Phi}_i + \mathbf{\Psi}_i + \mathbf{Z}_i)((\mathbf{\Gamma}_i^\dagger + \mathbf{\Phi}_i^\dagger + \mathbf{\Psi}_i^\dagger + \mathbf{Z}_i^\dagger)]\mathbf{C}_i^\dagger) \\
&= E[\text{tr}(\mathbf{C}_0(\mathbf{\Gamma}_0\mathbf{\Gamma}_0^\dagger + \mathbf{\Phi}_0\mathbf{\Phi}_0^\dagger + \mathbf{\Psi}_0\mathbf{\Psi}_0^\dagger + \mathbf{Z}_0\mathbf{Z}_0^\dagger)\mathbf{C}_0^\dagger)] \\
&+\text{tr}(\mathbf{C}_0(E[\mathbf{\Gamma}_0\mathbf{\Phi}_0^\dagger] + E[\mathbf{\Gamma}_0\mathbf{\Psi}_0^\dagger] + E[\mathbf{\Gamma}_0\mathbf{Z}_0^\dagger] + E[\mathbf{\Phi}_0\mathbf{\Psi}_0^\dagger] + E[\mathbf{\Phi}_0\mathbf{Z}_0^\dagger] + E[\mathbf{\Psi}_0\mathbf{Z}_0^\dagger])\mathbf{C}_0^\dagger) \\
&+E[2\sum_{i=1}^{L} \text{tr}(\mathbf{C}_i(\mathbf{\Gamma}_i\mathbf{\Gamma}_i^\dagger + \mathbf{\Phi}_i\mathbf{\Phi}_i^\dagger + \mathbf{\Psi}_i\mathbf{\Psi}_i^\dagger + \mathbf{Z}_i\mathbf{Z}_i^\dagger)\mathbf{C}_i^\dagger)] \\
&+\text{tr}(\mathbf{C}_i(E[\mathbf{\Gamma}_i\mathbf{\Phi}_i^\dagger] + E[\mathbf{\Gamma}_i\mathbf{\Psi}_i^\dagger] + E[\mathbf{\Gamma}_i\mathbf{Z}_i^\dagger] + E[\mathbf{\Phi}_i\mathbf{\Psi}_i^\dagger] + E[\mathbf{\Phi}_i\mathbf{Z}_i^\dagger] + E[\mathbf{\Psi}_i\mathbf{Z}_i^\dagger])\mathbf{C}_i^\dagger).
\end{aligned}
$$

When we take the expectation operation to the cross terms, the outputs are zero matrices, and it will be shown later. We thus get

$$
\begin{aligned}
&T_F = E[\text{tr}(\mathbf{C}_0(\mathbf{\Gamma}_0\mathbf{\Gamma}_0^\dagger + \mathbf{\Phi}_0\mathbf{\Phi}_0^\dagger + \mathbf{\Psi}_0\mathbf{\Psi}_0^\dagger + \mathbf{Z}_0\mathbf{Z}_0^\dagger)\mathbf{C}_0^\dagger)] \\
&+E[2\sum_{i=1}^{L} \text{tr}(\mathbf{C}_i(\mathbf{\Gamma}_i\mathbf{\Gamma}_i^\dagger + \mathbf{\Phi}_i\mathbf{\Phi}_i^\dagger + \mathbf{\Psi}_i\mathbf{\Psi}_i^\dagger + \mathbf{Z}_i\mathbf{Z}_i^\dagger)\mathbf{C}_i^\dagger)] \\
&= \Gamma_F + \Phi_F + \Psi_F + Z_F \\
&= G_F. \qquad \text{(A.1)}
\end{aligned}
$$

Now, we first prove $E[\mathbf{\Gamma}_i\mathbf{\Phi}_i^\dagger] = \mathbf{0}$ for $0 \le i \le L$. The $(a, b)$th of $\mathbf{\Gamma}_i$ are uncorrelated with

the noise ($\eta_j(n,k)$), and the $(a,b)$th entry of $\mathbf{\Gamma}_i\mathbf{\Phi}_i^\dagger$ can be expressed as

$$\sum_{l,s,i,j,n,k} f_{a,b}(h_{js}(l), d_i(n,k))\eta_j^*(n,k),$$
$$\text{for } 0 \le l \le L, 0 \le s, i \le M_t, 0 \le j \le M_r, 0 \le k \le N-1, 0 \le n \le Q-1$$

where $f_{a,b}(h_{js}(l), d_i(n,k))$ is a function of $h_{js}(l)$ and $d_i(n,k)$, and its output is related to the channel coefficients and the information symbols. Both of them are uncorrelated with the noise, so we get

$$\begin{aligned} E[\sum_{l,s,i,j,n,k} f_{a,b}(h_{js}(l), d_i(n,k))\eta_j^*(n,k)] &= \sum_{l,s,i,j,n,k} E[f_{a,b}(h_{js}(l), d_i(n,k))]E[\eta_j^*(n,k)] \\ &= 0\,. \end{aligned} \tag{A.2}$$

Since $E[\eta_j^*(n,k)] = 0$, we can obtain that each entry of $E(\mathbf{\Gamma}_i\mathbf{\Phi}_i^\dagger)$ is zero; In other words, it means $E(\mathbf{\Gamma}_i\mathbf{\Phi}_i^\dagger) = \mathbf{0}$ . By the similarly reason, we can get $E[\mathbf{\Gamma}_i\mathbf{\Psi}_i^\dagger] = \mathbf{0}$. Secondly , we prove $E[\mathbf{\Gamma}_i\mathbf{Z}_i^\dagger] = \mathbf{0}$. The $(a,b)$th of $\mathbf{\Gamma}_i$ can be expressed as

$$\begin{aligned} &\sum_{l,s,j,n_1\neq n_2,k_1,k_2,i_1,i2} f_{a,b}(h_{js}(l))d_{i1}(n_1,k_1)d_{i_2}^*(n_2,k_2) \\ &+ \sum_{l,s,j,n_1,n_2,k_1\neq k_2,i_1,i2} f_{a,b}(h_{js}(l))d_{i1}(n_1,k_1)d_{i_2}^*(n_2,k_2) \\ &+ \sum_{l,s,j,n_1,n_2,k_1,k_2,i_1\neq i2} f_{a,b}(h_{js}(l))d_{i1}(n_1,k_1)d_{i_2}^*(n_2,k_2) \\ &+ \sum_{l,s,j,n1,k1,i1} f_{a,b}(h_{js}(l))(d_{i_1}(n_1,k_1)d_{i1}^*(n_1,k_1) - 1), \\ &\text{for } 0 \le l \le L, 0 \le s, i_1, i_2 \le M_t, 0 \le j \le M_r, 0 \le k_1, k_2 \le N-1, 0 \le n_1, n_2 \le Q-1. \end{aligned}$$

The $(a,b)$th of $E[\mathbf{\Gamma}_i\mathbf{Z}_i^\dagger]$ can be expressed as

$$\begin{aligned} &\sum_{l,s,j,n_1\neq n_2,k_1,k_2,i_1,i_2} E[f_{a,b}(h_{js}(l),\eta_j(n,k))]E[d_{i_1}(n_1,k_1)d_{i_2}^*(n_2,k_2)] \\ &+ \sum_{l,s,j,n_1,n_2,k_1\neq k_2,i_1,i_2} E[f_{a,b}(h_{js}(l),\eta_j(n,k))]E[d_{i_1}(n_1,k_1)d_{i_2}^*(n_2,k_2)] \\ &+ \sum_{l,s,j,n_1,n_2,k_1,k_2,i_1\neq i_2} E[f_{a,b}(h_{js}(l),\eta_j(n,k))]E[d_{i_1}(n_1,k_1)d_{i_2}^*(n_2,k_2)] \\ &+ \sum_{l,s,j,n_1,k_1,i_1} E[f_{a,b}(h_{js}(l),\eta_j(n,k))]E[(d_{i_1}(n_1,k_1)d_{i_1}^*(n_1,k_1) - 1)] \\ &= 0 \end{aligned} \tag{A.3}$$

where $E[d_{i_1}(n_1,k_1)d_{i_2}^*(n_2,k_2)] = 0$ and $E[(d_{i_1}(n_1,k_1)d_{i_1}^*(n_1,k_1) - 1)] = 0$ . Thus, we can obtain $E[\mathbf{\Gamma}_i\mathbf{Z}_i^\dagger] = \mathbf{0}$. Thirdly, we prove $E(\mathbf{\Phi}_i\mathbf{\Psi}_i^\dagger) = \mathbf{0}$. The $(a,b)$th of $E(\mathbf{\Phi}_i\mathbf{\Psi}_i^\dagger)$ can

be expressed as

$$\begin{aligned}
&\sum_{l,s,j,n1\neq n2,k1,k2,i1,i2} E[f_{a,b}(h_{js}(l),\eta_j(n,k))]E[d_{i1}(n_1,k_1)d_{i2}(n_2,k_2)] \\
+&\sum_{l,s,j,n1,n2,k1\neq k2,i1,i2} E[f_{a,b}(h_{js}(l),\eta_j(n,k))]E[d_{i1}(n_1,k_1)d_{i2}(n_2,k_2)] \\
+&\sum_{l,s,j,n1,n2,k1,k2,i1\neq i2} E[f_{a,b}(h_{js}(l),\eta_j(n,k))]E[d_{i1}(n_1,k_1)d_{i2}(n_2,k_2)] \\
&+\sum_{l,s,j,n1,k1,i1} E[f_{a,b}(h_{js}(l),\eta_j(n,k))]E[(d_{i1}(n_1,k_1)^2)] \\
&= 0 \qquad \text{(A.4)}
\end{aligned}$$

where $E[d_{i1}(n_1,k_1)d_{i2}(n_2,k_2)] = 0$ and $E[d_{i1}(n_1,k_1)^2] = 0$ . Thus, we can obtain $E(\mathbf{\Phi}_i\mathbf{\Psi}_i^\dagger) = \mathbf{0}$. Lastly, we prove $E[\mathbf{\Phi}_i\mathbf{Z}_i^\dagger] = \mathbf{0}$, since the $(a,b)$th entry of $E[\mathbf{\Phi}_i\mathbf{Z}_i^\dagger]$ can be expressed as

$$\begin{aligned}
&\sum_{l,i,s,j,n,k} E[f_{a,b}(h_{js}(l),\eta_j(n,k))]E[d_i(n,k)] \\
&= 0 \qquad \text{(A.5)}
\end{aligned}$$

where $E[d_i(n,k)] = 0$. Thus, we can obtain $E[\mathbf{\Phi}_i\mathbf{Z}_i^\dagger] = \mathbf{0}$. By the similarly reason, we can get $E[\mathbf{\Psi}_i\mathbf{Z}_i^\dagger] = \mathbf{0}$.

# Bibliography


[1] W. Bai, C. He, L. ge Jiang, and H. wen Zhu. Blind channel estimation in mimo-ofdm systems. In *Global Telecommunications Conference, 2002. GLOBECOM '02. IEEE*, volume 1, pages 317 – 321 vol.1, 2002.

[2] H. Bolcskei, J. Heath, R.W., and A. Paulraj. Blind channel identification and equalization in ofdm-based multiantenna systems. *Signal Processing, IEEE Transactions on*, 50(1):96 – 109, Jan. 2002.

[3] Y.-S. Chen. Semiblind channel estimation for mimo single carrier with frequency-domain equalization systems. *Vehicular Technology, IEEE Transactions on*, 59(1):53 –62, 2010.

[4] Y.-S. Chen and C.-A. Lin. Blind identification of mimo channels in zero padding block transmission systems. *Signal Processing, IEEE Transactions on*, 55(2):764 –772, 2007.

[5] A. Chevreuil, E. Serpedin, P. Loubaton, and G. Giannakis. Blind channel identification and equalization using periodic modulation precoders: performance analysis. *Signal Processing, IEEE Transactions on*, 48(6):1570 –1586, June 2000.

[6] F. Gao and A. Nallanathan. Blind channel estimation for mimo ofdm systems via nonredundant linear precoding. *Signal Processing, IEEE Transactions on*, 55(2):784 –789, 2007.

[7] C. A. Lin and J. Y. Wu. Blind identification with periodic modulation: a time-domain approach. *Signal Processing, IEEE Transactions on*, 50(11):2875 – 2888, Nov. 2002.

[8] A. PAULRAJ, D. GORE, R. NABAR, and H. BOLCSKEI. An overview of mimo communications - a key to gigabit wireless. *Proceedings of the IEEE*, 92(2):198 – 218, Feb. 2004.

[9] E. Serpedin and G. Giannakis. Blind channel identification and equalization with modulation-induced cyclostationarity. *Signal Processing, IEEE Transactions on*, 46(7):1930 –1944, July 1998.

[10] C. Shin, R. Heath, and E. Powers. Non-redundant precoding-based blind and semi-blind channel estimation for mimo block transmission with a cyclic prefix. *Signal Processing, IEEE Transactions on*, 56(6):2509 –2523, 2008.

[11] B. Su and P. P. Vaidyanathan. Research article a generalized algorithm for blind channel identification with linear redundant precoders, 2006.

[12] J.-Y. Wu and T.-S. Lee. Periodic-modulation-based blind channel identification for single-carrier block transmission with frequency-domain equalization. *Signal Processing, IEEE Transactions on*, 54(3):1114 – 1130, 2006.

[13] J.-Y. Wu and T.-S. Lee. Nonredundant precoding-assisted blind channel estimation for single-carrier space ndash;time block-coded transmission with frequency-domain equalization. *Signal Processing, IEEE Transactions on*, 55(3):1062 –1080, 2007.

[14] Y. Zeng, Y.-C. Liang, and C. Xu. Semi-blind channel estimation for linearly precoded mimo-cpsc. In *Communications, 2008. ICC '08. IEEE International Conference on*, pages 604 –608, May 2008.

[15] Y. Zeng and T.-S. Ng. A semi-blind channel estimation method for multiuser multiantenna ofdm systems. *Signal Processing, IEEE Transactions on*, 52(5):1419 – 1429, May 2004.